Review

Recent Progress in Self-Powered Sensor Based on Liquid-Solid Triboelectric Nanogenerator

Quang Tan Nguyen , Duy Linh Vu , Chau Duy Le , Kyoung Kwan Ahn *

Posted Date: 1 June 2023

doi: 10.20944/preprints202306.0006.v1

Keywords: Self-powered sensor; flexibility sensor; triboelectric nanogenerator; liquid-solid interface; active sensor; chemical sensor

Review

Recent Progress in Self-Powered Sensor Based on Liquid-Solid Triboelectric Nanogenerator

Quang Tan Nguyen [1], Duy Linh Vu [2], Chau Duy Le [3,4] and Kyoung Kwan Ahn [2,*]

[1] Graduate School of Mechanical Engineering, University of Ulsan, Daehakro 93, Nam-gu, Ulsan, 44610, South Korea; paxnguyen91@ulsan.ac.kr
[2] School of Mechanical Engineering, University of Ulsan, Daehakro 93, Nam-gu, Ulsan, 44610, South Korea; dlinh5832@ulsan.ac.kr
[3] Faculty of Electrical and Electronic Engineering, Ho Chi Minh University of Technology (HCMUT), 268 Ly Thuong Kiet Street, District 10, Ho Chi Minh City, 700000, Vietnam
[4] Vietnam National University Ho Chi Minh City, Linh Trung Ward, Thu Duc City, Ho Chi Minh City, 700000, Vietnam; lechauduy@hcmut.edu.vn
* Correspondence: kkahn@ulsan.ac.kr

Abstract: Recently, there is a growing need for sensors that can operate autonomously, without the need for an external power source. This is especially important in applications where conventional power sources, such as batteries, are impractical or difficult to replace. Self-powered sensors have emerged as a promising solution to this challenge, offering a range of benefits such as low cost, high stability, and environmental friendliness. One of the most promising self-powered sensor technologies is L-S TENG, which stands for the liquid-solid triboelectric nanogenerator. This technology works by harnessing the mechanical energy generated by external stimuli such as pressure, touch, or vibration, and converting it into electrical energy that can be used to power sensors and other electronic devices. Therefore, self-powered based on L-S TENG, which provides numerous benefits such as rapidly responding, portability, cost-effectiveness, and miniaturization, is critical for increasing living standards and optimizing industrial processes. In this review paper, the working principle with three basic modes has been briefly introduced firstly. After that, affecting parameters to L-S TENG are reviewed based on the properties of the liquid and solid phases. With different working principles, L-S TENG has designed a lot of structure that works as a self-powered sensor for pressure/force change, liquid flow motion, concentration, and chemical detection or biochemical sensing. Moreover, the continuous output signal of TENG plays an important role in a real-time sensor that is vital to the growth of the Internet of Things.

Keywords: self-powered sensor; flexibility sensor; triboelectric nanogenerator; liquid-solid interface; active sensor; chemical sensor

1. Introduction

Over the past few years, the challenges posed by climate change and energy shortages have become increasingly extreme, thereby highlighting the pressing need for clean and renewable energy[1]. Despite the vast amounts of energy contained within human footfalls, ocean waves, raindrops, and airflow, a significant portion of it is wasted due to the difficulty of harnessing it effectively[2,3]. Therefore, it is crucial to develop suitable technology to tap into this energy source, and advancements in nanotechnology have led to the creation of various nanogenerators for harvesting mechanical energy[4–6]. Wang and his team developed triboelectric nanogenerators (TENGs) which use the electrostatic and triboelectrification effects to turn mechanical energy into electricity [7]. TENGs are capable of generating electricity from various energy sources, including vibration, wind, wave water, and human motion, among others [8–11]. Since their inception, researchers have studied various TENG structures and functions to enhance their output performance and energy conversion efficiency[12–15].

Aside from the extraordinarily rapid development of solid-solid TENG [16–18], liquid-solid TENG (L-S TENG) has also been becoming a potential trend due to its stable output and durability

Preprints (www.preprints.org) | NOT PEER-REVIEWED | Posted: 1 June 2023 doi:10.20944/preprints202306.0006.v1

[19–24]. The L-S TENG device has been developed based on a simple concept that water drops contact the dielectric solid surface and generate electricity. For example, the metal liquid was used for the TENG device and can harvest energy with a high conversion efficiency of 70.6 % [25]. Waves energy has been recovered by using the flexible L-S TENG, it is considered a power supply solution anywhere as long as wave energy is available [26]. Electricity was generated from L-S TENG devices when water flows through the elastic silicon tubing [27]. Although the exact electrostatic effect is still unclear, the working principle of liquid contact with solid has been tried to explain by the movement of the triboelectric charge on the surface of the materials.

L-S TENG can be used in specific applications depending on the type of liquid-solid contact. A collection of photographs of L-S TENG used for energy harvesting and self-powered sensors is shown in Figure 1 [28–33]. Energy harvesting from tidal and oceanic waves, rainfall, and water streams offers enormous promise for L-S TENG. The L-S TENG gadget has been successfully used in self-powered sensors in recent years because of its capacity to transform mechanical energy into electric output without the need for a power unit. The L-S TENG gadget has been successfully used in self-powered sensors in recent years because of its capacity to transform mechanical energy into electricity without the need for a power unit. As a result, this review concentrates on the most current developments in self-powered sensors based on L-S TENG, as well as their practical applications. The review begins with a description of the L-S TENG basic operation and various operating modes, followed by a summary of the variables that affected it. Secondly, a range of self-powered sensors based on L-S TENG such as active pressure/touch sensors,[31] chemical sensors [34], biological sensors [35], gases sensing [36,37], and so on will be summarized as strong applications for TENG devices. Finally, the conclusion section highlights future opportunities and perspectives for the development of self-powered sensors based on L-S TENG.

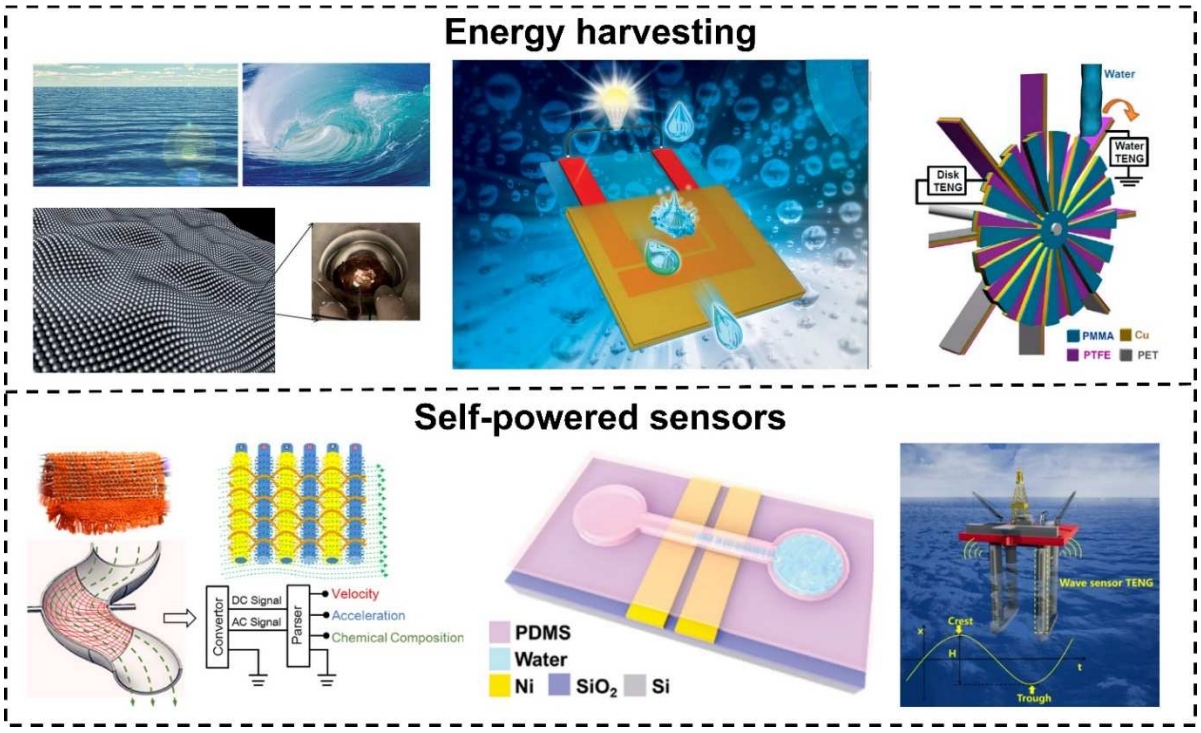

Figure 1. Application of L-S TENG in energy harvesting and self-powered sensors. Reproduced with permission from Reference [28] 2014, Royal Society of Chemistry; Reference [29] 2014, Royal Society of Chemistry; Reference [30] 2014, American Chemical Society; Reference [31] 2018, American Chemical Society; Reference [32] 2016, Wiley; and Reference [33] 2019, Elsevier.

Preprints (www.preprints.org) | NOT PEER-REVIEWED | Posted: 1 June 2023 doi:10.20944/preprints202306.0006.v1

2. Liquid-Solid Contact Triboelectric Nanogenerator

2.1. Mechanism of Liquid-Solid Contact Electrification

Contact electrification (CE) is a fundamental phenomenon in electricity generation that occurs when two materials are physically in contact and friction with each other, as a result of tribology and interfacial charge transfer [38]. The exact mechanism behind the transfer of charges has been a topic of debate for many years without a definitive conclusion. In an attempt to explain CE at the atomic level, Wang et al. [39] proposed the interatomic interaction model, also called the Wang transition. Accordingly, the dominant mechanism for CE is suggested to be electron transfer. As depicted in Figure 2a, CE can occur at contact interfaces between solids, liquids, and gases.

When two atoms form a bond, an equilibrium interatomic distance is established. If the distance is shortened by an externally applied force, the atoms will repel each other due to increased electron cloud overlap. Conversely, if the distance is longer, the atoms will attract due to decreased overlap, as shown in Figure 2b. Furthermore, Wang et al. [39] found that CE only occurs when the distance is forced shorter than the equilibrium distance, allowing for electron transfer and static charges on material surfaces. The electrostatic charges are released through thermal ionic emission or photon excitation. The Wang transition model explains the occurrence of liquid-solid CE, which happens when liquid molecules collide with solid surface atoms under liquid pressure, leading to electron transfer and electron cloud overlap [40]. To further understand, Wang et al. [39] proposed a "two-step" model for the formation of the electric double layer (EDL), with electron transfer playing a dominant role in the first step. As shown in Figure 2c, when a liquid contacts a solid surface, electron cloud overlap can cause electron transfer and charge the solid surface. Under liquid flow pressure, ions attach to the surface, forming a layer with freely migrating ions in the liquid. Positive ions, attracted by electrostatic interactions, migrate toward the surface and form an EDL in the second step. CE due to electron transfer likely initiates the formation of the EDL [41].

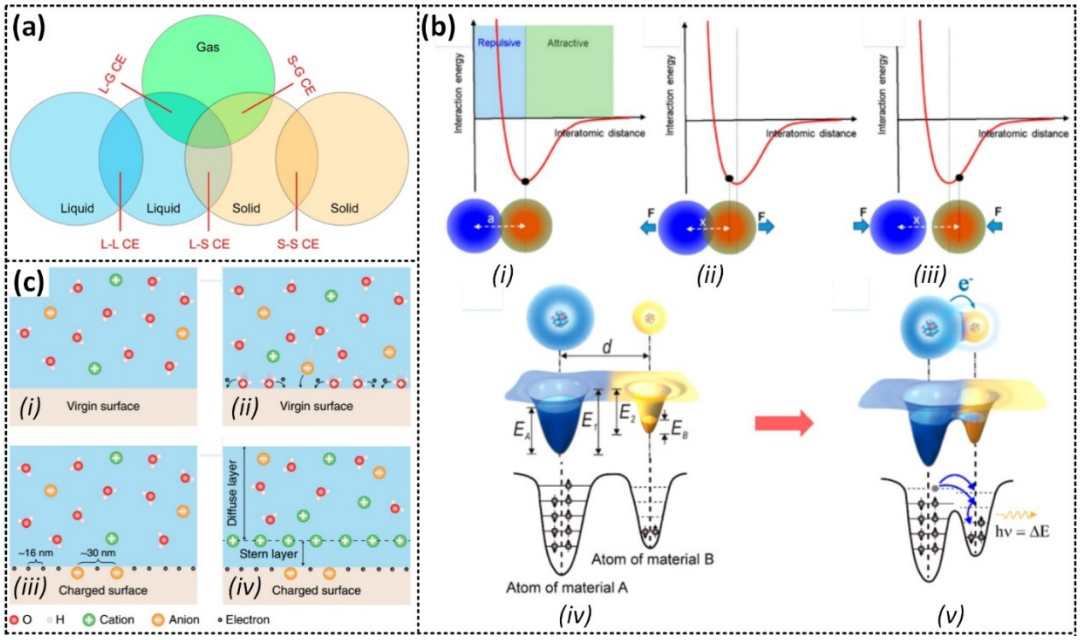

Figure 2. (a) Schematic of the contact electrification between different phases. (b) Interaction of two atoms. (c) Mechanism of contact electrification at the liquid-solid interface and formation of the EDL. Reproduced with permission from Reference [40] 2022, American Chemical Society; Reference [41] 2020, Wiley.

2.2. Basic Mode of Operation of Liquid-Solid Triboelectric Nanogenerator

A liquid-solid triboelectric nanogenerator (L-S TENG) is a highly efficient device capable of converting different types of mechanical energy into electrical energy, with a particular focus on

 doi:10.20944/preprints202306.0006.v1

applications involving flowing water. This is achieved through the coupling effects of liquid-solid CE and electrostatic induction. Previous research has identified four distinct modes of operation for L-S TENG, which are determined by the movement of the triboelectric layer and the configuration of the electrodes. These modes include contact separation [43–46], lateral sliding [47–49], free-standing [19,20,50–63], and single electrode [15,33,64–73] modes.

2.2.1. Contact-Separation Mode

In the contact-separation mode of L-S TENG, electrical energy is produced through electrical induction, which occurs when a solid surface oscillates vertically and makes contact with water before separating from it [43–46]. As can be seen in Figure 3a, Lin et al. [43] reported a water-TENG based on this principle, which achieved a voltage of 52 V, and current and power densities of about 2.45 mA/m^2 and 0.13 W/m^2, respectively. Before contact, the polydimethylsiloxane (PDMS) surface remains uncharged and no charge transfer occurs between PDMS and water (Figure 3a-i). However, when the PDMS surface comes into contact with water under external pressing force, CE occurs, generating a negatively charged PDMS surface and a positively charged EDL (Figure 3a-ii). Once the PDMS separates from the water, the transferred charges remain on the PDMS surface, breaking the electrical neutrality and establishing a difference in electric potential. This leads to inducing positive and negative charges on the corresponding electrodes to balance the potential difference. As a result, electrons flow from Cu electrode 2 to Cu electrode 1, generating a current in the external circuit (Figure 3a-iii). The current output obtains the maximum when PDMS returns to the initial position (Figure 3a-iv). When the PDMS is forced to get closer and then contact again with the water surface, the potential difference decreases, causing a reverse flow of electrons and generating a current in the opposite orientation (Figure 3a-v). Once a new equilibrium state is established, the device returns to its initial state, and no current is generated. Due to the periodic contact separation of PDMS and water, the TENG provides a continuous output through the external circuit with alternating current characteristics.

Similarly, a liquid-solid-based triboelectric generator (LSTEG) was proposed by Yang et al. [46], which can produce a significant amount of power with a power density of 9.62 W/m^2. The working mechanism of LSTEG is illustrated in Figure 3b, where contact between PTFE and water generates triboelectric charges on their surfaces (Figure 3b-ii). As PTFE separates from the water surface, the negatively charged PTFE surface induces positive charges on Cu electrode 1, while negative charges are induced on Cu electrode 2 (Figure 3b-iii), generating a positive current flow through the external circuit until the PTFE returns to the initial position (Figure 3b-iv). When PTFE is pressed into contact again with the water, a reverse current flow occurs until a new equilibrium state is reached (Figure 3b-v). It is clear that one press-release cycle of PTFE can produce an alternating current.

Preprints (www.preprints.org) | NOT PEER-REVIEWED | Posted: 1 June 2023 doi:10.20944/preprints202306.0006.v1

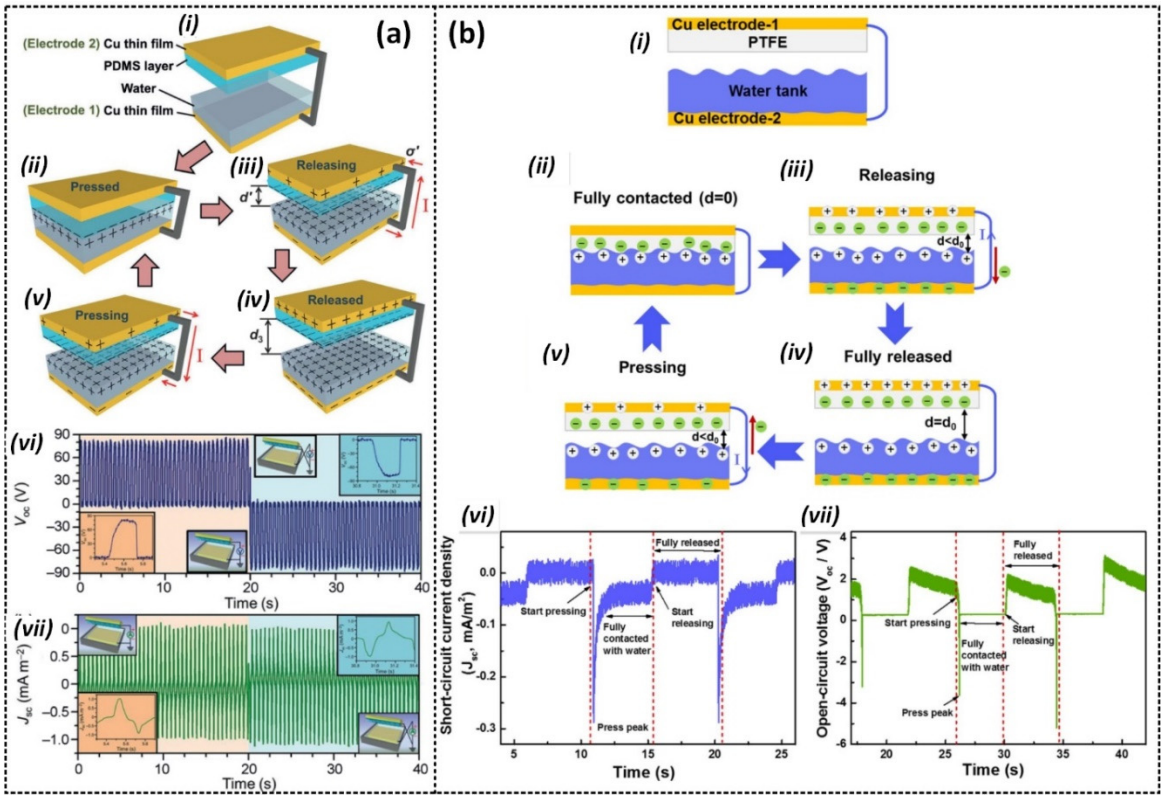

Figure 3. Schematic diagram and working mechanism of (a) the water-TENG proposed by Lin et al. [43] and (b) the LSTEG proposed by Yang et al. [46]. Reproduced with permission from Reference [43] 2013, Wiley; Reference [46] 2018, Elsevier.

2.2.2. Lateral Sliding Mode

Lateral sliding mode is another power generation mode that utilizes the same structure as the contact separation mode but with a different manner of movement. Instead of relying on contact separation, it produces power through lateral movement between two contact surfaces, where relative friction plays a crucial role [47–49]. The working mechanism of a lateral sliding mode L-S TENG is illustrated in Figure 4a. Nahian et al. [48] proposed a lateral sliding-style fluid-based triboelectric nanogenerator (L-S FluTENG), which consists of an aluminum tape covered by a PTFE layer and located on the outer surface of a tube, and a cylindrical reservoir with a Cu located on the inside surface. Initially, the PTFE and water surfaces are uncharged (Figure 4a-i). When the PTFE slides are immersed in the water, CE occurs at the contact interface, resulting in positively and negatively charged water and PTFE surfaces, respectively (Figure 4a-ii). Next, once the PTFE emerges from the water, the charge balance is broken, and electrons are attracted to flow from the aluminum electrode to the copper electrode to neutralize the unbalanced charges, producing a current through the external circuit until completely separate from the water (Figure 4a-iii). Subsequently, when the PTFE slides immersed again in the water, the positive water forms an interfacial EDL with the PTFE (Figure 4a-iv). Electrons will flow inversely to neutralize the charged electrodes. This figure also displays the voltage and current outputs of LS-FluTENG, which proves its AC characteristics, with a peak voltage of 6 V and peak current of 300 nA. In the contact-separation mode of L-S TENG, electrical energy is produced through electrical induction.

In addition, Lee et al. [47] reported a water-based TENG, in which an Al plate covered by Teflon AF 1600 (PTFE) periodically slides immersed/emerged into/out of the water, as depicted in Figure 4b. When the PTFE and water are in physical contact, CE occurs, leading to generating negatively and positively charged PTFE and water surfaces, respectively. Once the PTFE emerges from the water, charged PTFE and water surfaces induce positive and negative charges on the Al and Cu electrodes, leading to generating a current flow through the external circuit, and maximizing when the PTFE is

Preprints (www.preprints.org) | NOT PEER-REVIEWED | Posted: 1 June 2023 doi:10.20944/preprints202306.0006.v1

completely out of the water. When the PTFE immerses in the water again, a current flow with an inverse direction is generated in the external circuit. Therefore, the periodic slides immersed/emerged into/out of the water can produce alternating currents. This is confirmed experimentally by the voltage and current outputs generated by WTENG at a movement frequency of 2 Hz.

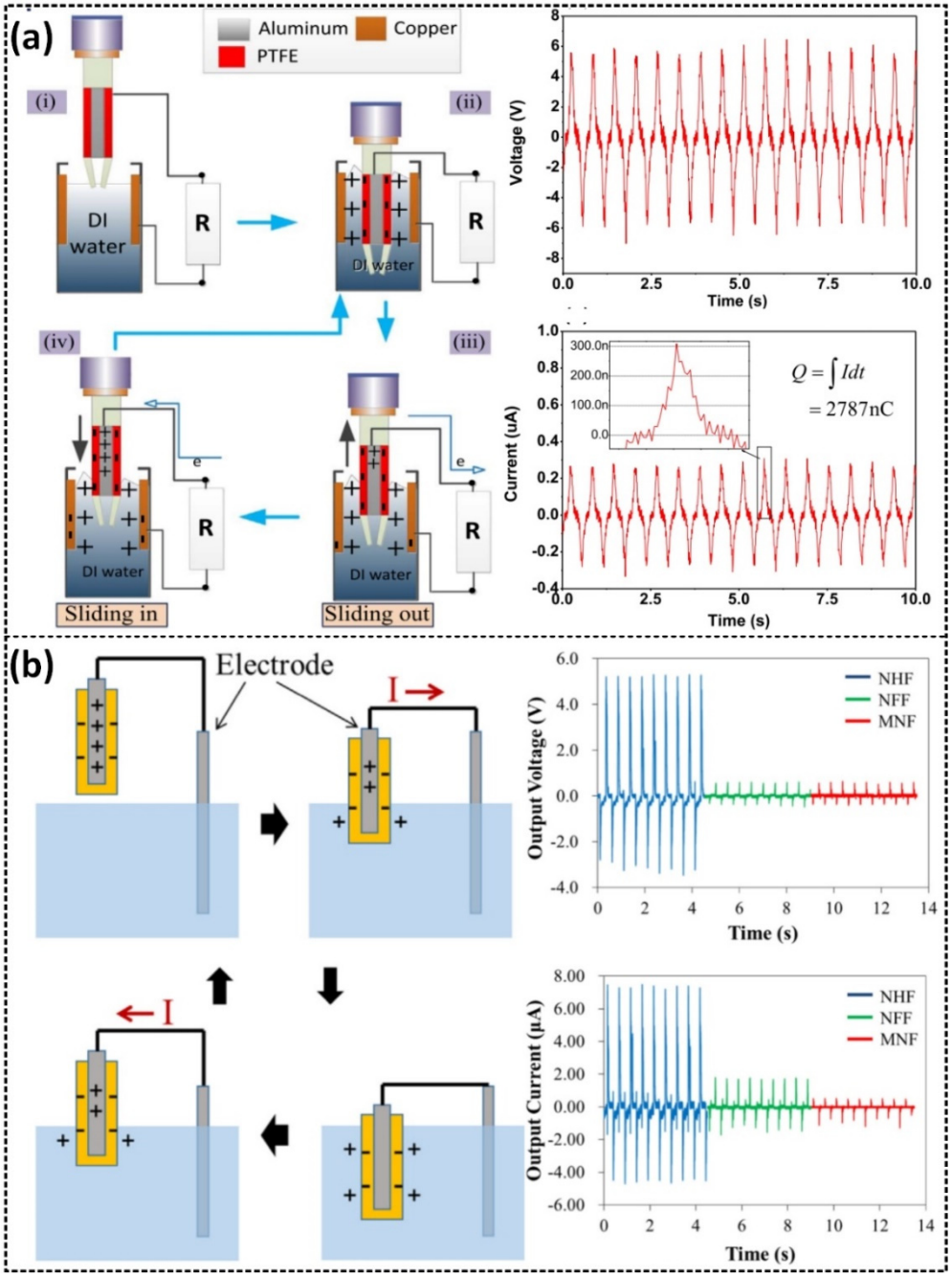

Figure 4. Working mechanism and the comparison of the measured results of open-circuit voltage and short-circuit current of (a) the L-S FluTENG and (b) the WTENG. Reproduced with permission from Reference [48] 2017, Elsevier; Reference [47] 2018, Elsevier.

2.2.3. Free-standing Mode

The typical free-standing mode of TENG involves a free-moving triboelectric object and two electrodes [19,20,50–63]. For instance, Kim et al. reported a rotating water TENG that can generate a maximum instantaneous open-circuit voltage of 27.2 V and a short-circuit current of 3.84 μA [56]. The step-by-step mechanism of the device is illustrated in Figure 5a. This device consists of PTFE-coated Al electrodes positioned on the inner surface

Preprints (www.preprints.org) | NOT PEER-REVIEWED | Posted: 1 June 2023 doi:10.20944/preprints202306.0006.v1

of a cylinder, which is partially filled with water. The CE occurring at the contact interface of the water and PTFE leads to producing AC outputs. During the rotation, the water gradually deforms under the effect of gravity and dynamic inertia. On the other aspect, electrodes E1 and E2 located on the opposite side of the cylinder are connected. In stage (i), E1 and E2 establish an electrical equilibrium state. As E1 emerges out of the water and E2 contacts water due to the rotation of the cylinder, the equilibrium state is disrupted, creating a unbalance potential between the water and PTFE, leading to current flow through the external circuit. Once E2 fully contacts the water, a new equilibrium state forms. CE continuously occurs between the water and PTFE, and the electrostatic induction process induces an inverse current flow in the external circuit. Both voltage and current outputs exhibit AC characteristics. Another example is the U-shaped TENG constructed by Zhang et al. [20]. This device comprises an FEP U-shaped tube, two Cu electrodes located on the outer surface of two columns of the FEP U-shaped tube, and partially filled water (Figure 5b). The continuous up-and-down flow of water along the left and right columns generates electrostatic charges due to the CE of water and FEP, leading to electrical energy generation via electrostatic induction on two electrodes. The device can produce a peak voltage of 20 V and a peak current of 400 nA.

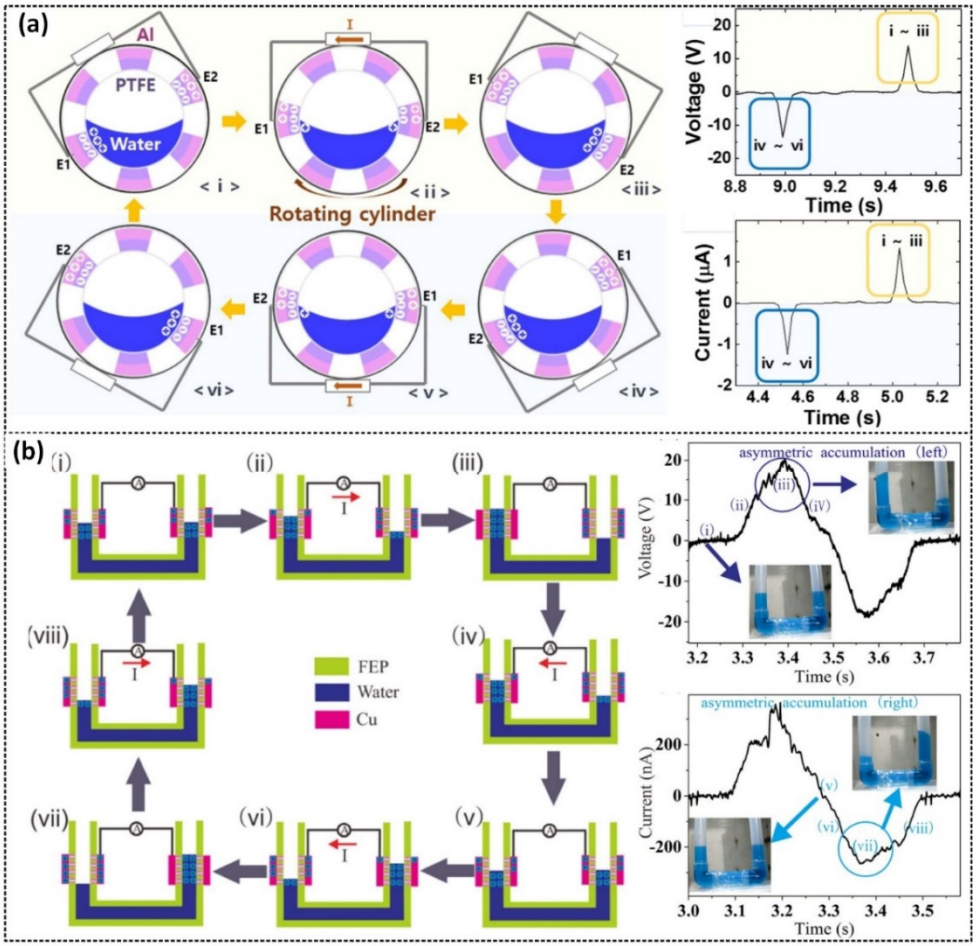

Figure 5. Working mechanism and typical voltage and current output signals of (a) the rotating water TENG and (b) the U-shaped TENG. Reproduced with permission from Reference [56] 2016, Elsevier; Reference [20] 2017, Elsevier.

2.2.4. Single-electrode Mode

Another important mode of operation of L-S TENG is the single-electrode mode that generates electricity through a single-electrode connected to the ground. Compared to the other modes such as

Preprints (www.preprints.org) | NOT PEER-REVIEWED | Posted: 1 June 2023 doi:10.20944/preprints202306.0006.v1

contact separation, lateral sliding, and free-standing modes, which generate electricity due two the electrostatic induction process between two electrodes, a single-electrode-based L-S TENG has several advantages [15,33,64–73].

Lin et al. demonstrated a water-TENG with a superhydrophobic PTFE surface, working in a single-electrode mode, that can convert the energy from flowing water and falling droplets (Figure 6a) [15]. This device can generate a maximum voltage and current of 9.3 V and 17 μA, respectively, from a water droplet of about 30-μL. When a water droplet falls onto the surface of a PTFE thin film, CE occurs at the water-PTFE interface, resulting in generating a negatively charged PTFE surface and a positive EDL, and electrical equilibrium is formed. Once the water droplet spreads out from the PTFE, the electrical equilibrium is broken leading to the development of a potential difference across the Cu electrode and the ground, driving the current flow in the external circuit. Electrons from the Cu electrode flow to the ground until reaching equilibrium, generating a negative current. When other water droplet contacts the PTFE surface, the negatively charged PTFE surface attract the positive ions inside the droplet to form an EDL, establishing an unbalance potential between the Cu electrode and the ground. Electrons are attracted to flow from the ground, generating a positive current through the external circuit. In the case that the droplet leaves the PTFE film, an inverse current is obtained until achieving another new equilibrium. Consequently, the periodic falling of water droplets exhibits a continuous AC output. Yang et al. also presented a similar study in which a water droplet-driven TENG (Wd-TENG) demonstrated that positive and negative current peaks can be generated during the contact separation of a falling droplet and a triboelectric layer surface [66]. The working mechanism of Wd-TENG and its typical current signal concerning the droplet's motion is shown in Figure 6b.

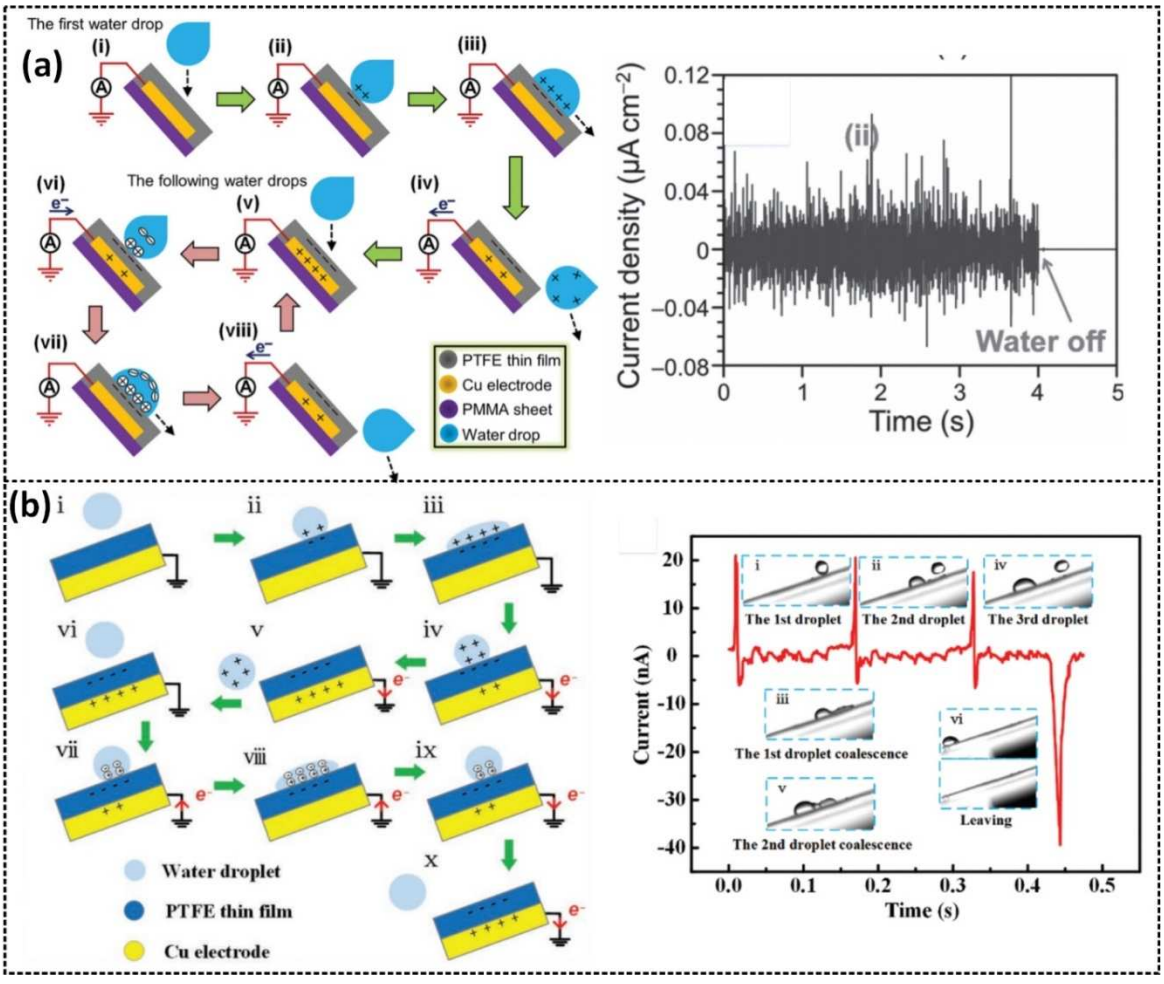

 doi:10.20944/preprints202306.0006.v1

Figure 6. Working mechanism and typical output current signal of (a) water-TENG with a superhydrophobic PTFE surface and (b) the Wd-TENG. Reproduced with permission from Reference [15] 2014, Wiley; Reference [66] 2019, Wiley.

2.3. Interacting Modes of Liquid-Solid Triboelectric Nanogenerator

The L-S TENG provides a promising technology for harvesting mechanical energy from liquid flow into electricity. Based on the source of the liquid dynamics, the L-S TENG can be divided into three main modes, including droplet [15,42,45,53–55,60,61,63,64,66–69,71,72,74–80], wave [33,44,49–52,56,59,65,81–83], and flow-based [19,20,58,62,73,84] modes. The most important source for L-S TENGs is the water, which exists everywhere in nature with an enormous amount, such as raindrops, rivers, tides, and ocean waves. Therefore, the interaction modes of L-S TENG will be reported in the following sections based on the water-TENG.

2.3.1. Droplet-based L-S TENG

Droplet-based mechanisms are commonly used in L-S TENGs to harvest energy from falling droplets or raindrops, which interact with a charge-generating layer and induce charges on the electrodes and generate a current in an external circuit. The charge-generating layer could be an insulator [15,42,45,53–55,60,61,64,66–69,71,72,76–80], semiconductor [23,63,75,85–87], or conductor [74] material. Lee et al. proposed a water droplet-driven TENG (WdTENG) that works in the contact-separation mode, where a water droplet bounces between two superhydrophobic surfaces made by a typical negative triboelectric material, PTFE, as shown in Figure 7a [45]. This device can generate peak voltage and current of about 6.8 V and 6 μA, respectively, measured at an inclination angle of 70°. Lu et al. reported an LS-TENG that converts energy from the movement of a water droplet between two semiconductors with different Fermi levels (Figure 7b) [63]. This device exhibits peak voltage and current of 0.3 V and 0.64 μA, respectively, with DC characteristics. Unlike conventional TENGs, which normally produce AC outputs, this study proved a new approach for harvesting low-frequency vibration energy directly into DC power. It also highlighted the potential for integrated and miniaturized generators, as the output characteristics of the device can be determined by relative parameters such as the speed, direction, and volume of the water droplet.

Moreover, for enhancing the output performance, various affecting parameters have been investigated, including the selection of triboelectric materials and the device concept. Traditionally, the droplet-based mechanism uses one or two electrodes covered by an insulator, where charges generated by the friction energy of water and the triboelectric layer remain on the solid surface after the separation of water from the layer. This induces the electrostatic charges to flow between two electrodes (double-electrodes mode) or between one electrode and the ground (single-electrode mode). Accordingly, these devices typically generate AC electricity [15,42,54,55,60,66,69,79].

Recently, a new methodology of electricity generation has emerged based on a new electrode structure design. In this design, the charge generated due to CE between water and the triboelectric layer will directly transfer to the electrode when the charge-carried water droplet directly contacts the electrode [67,68,72,76–78,80]. This leads to a different electrical response compared to traditional droplet-based TENGs. For example, Xu et al. proposed a droplet-based device using PTFE with a tiny piece of aluminum deposited onto a glass substrate with an ITO electrode underneath [80]. This device can output high values of instantaneous voltage and current of 143.5 V and 270.0 μA, respectively, which are much higher than those generated in the case without using an Al electrode. Wang et al. reported a similar device (SHS-DEG) consisting of structurally hierarchical and superhydrophobic FEP with a Cu electrode underneath the FEP film and an aluminum electrode located on the FEP surface (Figure 7c) [68]. SHS-DEG can produce a peak voltage of about 200 V and a peak current of 400 μA.

Preprints (www.preprints.org) | NOT PEER-REVIEWED | Posted: 1 June 2023 doi:10.20944/preprints202306.0006.v1

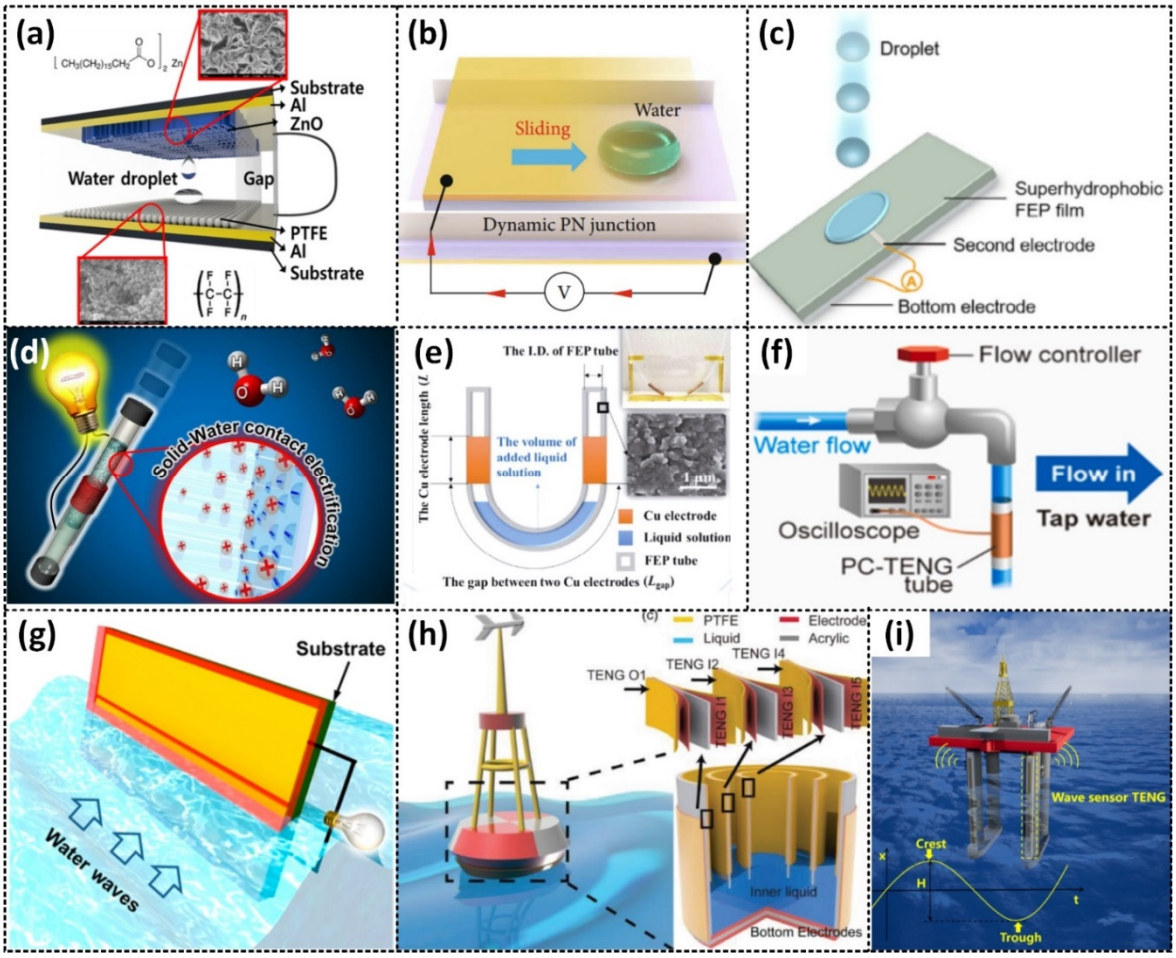

Figure 7. Schematic diagrams of (a-c) the droplet-based, (d-f) flow-based, and (g-i) wave-based L-S TENGs. Reproduced with permission from Reference [45] 2019, Elsevier; Reference [63] 2021, Science Partner Journals; Reference [68] 2021, Wiley; Reference [62] 2015, Springer Nature; Reference [19] 2018, Springer Nature; Reference [73] 2022, Elsevier; Reference [51] 2014, American Chemical Society; Reference [65] 2018, Wiley; Reference [33] 2018, Elsevier.

2.3.2. Flow-based LS-TENG

Another important interacting mode of L-S TENG is the continuous CE that occurs at the contact interface of a streaming flow liquid and a solid surface [19,20,58,62,73,84]. This mode of interaction allows for the conversion of mechanical energy from the flow of water into electrostatic energy. This electrostatic energy is then converted into electricity through either electrostatic induction [19,20,58,62,73] or the breakdown effect [84]. One example of this is the SWING stick developed by Choi et al., which converts the mechanical energy from shaking into electricity (Figure 7d) [62]. The stick generates electricity through CE between the water and Teflon, creating positive charges inside the water and negative charges on the Teflon surface. When the charged water contacts the bare Al tube, the generated charges inside the water are neutralized, generating a current through the external circuit. Other examples include the U-tube TENG developed by Zhang et al. [20] and Pan et al. [19] (Figure 7e), which can generate stable peak output voltage and current of about 20 V – 400 nA, and 350 V – 1.75 μA, respectively [20]. These devices can also function as multifunctional sensors, such as displacement and pressure sensors, with high sensitivity. Another example is the PTFE-copper (PCTENG) tube developed by Munirathinam et al. (Figure 7f) [73], which can harvest energy from flowing water and achieve peaks voltage, current, and power of 36 V, 0.8 μA, and 45 μW, respectively. The electricity is generated through CE occurring between the flowing water and the PTFE tube.

 doi:10.20944/preprints202306.0006.v1

2.3.3. Wave-based LS-TENG

Compared with the droplet and flow-based L-S TENG, wave-based L-S TENG also received significant attention from scientists due to the large amount of energy contained in the dynamic waves. In a recent study, Zhu et al. [51] reported the development of an LSEG using FEP thin film with an array of electrodes underneath (Figure 7g). The LSEG generates AC electricity by combining triboelectrification and electrostatic induction during traveling water waves. This study demonstrated the use of the LSEG as an effective energy harvester from ambient water waves and also showed the potential of the LSEG in both onshore and offshore areas, as well as rainy areas applications, contributing an important and promising solution for the sustainable development of society. Li et al. designed a buoy LS-TENG, that can output a high current and voltage of 290 μA and 300 V by synchronizing the outputs of a network of 18 LS-TENGs (Figure 7h) [65]. The produced energy is suitable to power a wireless SOS system for ocean emergencies. Importantly, wave-based LS-TENG also demonstrated its potential to be used in self-powered sensor systems. Xu et al. developed an L-S TENG that can be served as a wave height sensor for smart marine equipment (Figure 7i) [33].

3. Affecting parameter on L-S TENG performance

Studying the affecting parameters of L-S TENGs is a complex and challenging task due to the diverse device designs and working modes involved. Nonetheless, ongoing research is actively addressing this challenge by focusing on the factors that impact the output performance and durability of L-S TENG devices. The liquid phase and solid phase are the two major groups into which these influencing factors can be divided. Liquid phase parameters include elements like the type of liquid, viscosity, and surface tension, all of which can affect how well L-S TENG performs. Meanwhile, solid phase properties refer to the type of solid material used, surface morphology, and structure shape, which can also affect the output of these devices. Therefore, understanding these affecting parameters and developing methods to optimize the output performance and durability of L-S TENGs are essential for their widespread adoption. Despite the challenges associated with studying L-S TENGs, the potential benefits of this technology make it a promising field of research. By gaining a better understanding of the affecting parameters of L-S TENGs, researchers can work towards developing more efficient and durable devices that can be utilized in a broad range of applications.

The solid phase of an L-S TENG consists of two essential components: the contact layer and the electrode layer. The first consideration is the electrode layer, as the choice of materials for this layer is critical to the performance of the device. The selected material with high electrical conductivity can significantly enhance the electronic transfer from the contact layer, leading to a more efficient output performance. In addition to conductivity, flexibility is also an important factor when fabricating TENG devices with various models. Over the last few years, several materials, including aluminum, silver, gold, and copper, have been commonly used as electrode materials in L-S TENG devices. These materials possess high conductivity, good flexibility, commercial availability, and well-researched properties, making them ideal for TENG fabrication. Therefore, selecting the appropriate electrode material is crucial in the design and performance of L-S TENG devices. Through careful selection and utilization of materials, researchers can continue to improve the output performance and durability of TENGs and expand their potential applications [88–91]. Moreover, a lot of other conductive material has been proposed due to their common flexible, stretchable properties and high chemical stability including carbon nanotubes (CNTs) [92,93], graphene [94], nanowire-based materials [95], organic or polymer-based materials [96].

Apart from the electrode layer, the contact or hydrophobic layer plays a role important in increasing the TENG output. Due to the positive triboelectric properties of the liquid, the contact layer material should have high negatively charged. To quantitatively standardize the triboelectric effect, the triboelectric charge density (TECD) was measured to rank materials (Figure 8) [97]. In a triboelectric series, some common material has been used with low TECD such as PVC, PTFE, PDMS, Kapton, and PVDF equivalent to TECD value -117.5, -113.1, -102.2, -92.9, and -87.4 $mC.m^{-2}$,

Preprints (www.preprints.org) | NOT PEER-REVIEWED | Posted: 1 June 2023 doi:10.20944/preprints202306.0006.v1

respectively [97]. Besides that, the negative charge of material can be increased by using corona discharging of the air through using the air-ionization gun. After using corona discharging, the TECD could increase more than 5 times compared to the initial material [98]. The hydrophobic surface has also been researched a lot in improving output performance. Several ways have been used to a fabricated high hydrophobic surfaces such as nanostructures or hierarchical structures [71], artificial lotus leaf structures [53], and plasma treatment [99]. It is noteworthy that the surface morphology of the contact layer affects the velocity of the liquid on the contact layer and the bouncing motion between the liquid-solid surface. The hydrophobic surface is characterized by contact and sliding angle. High contact and sliding angle will increase the current output in the droplet single-electrode contact mode [45].

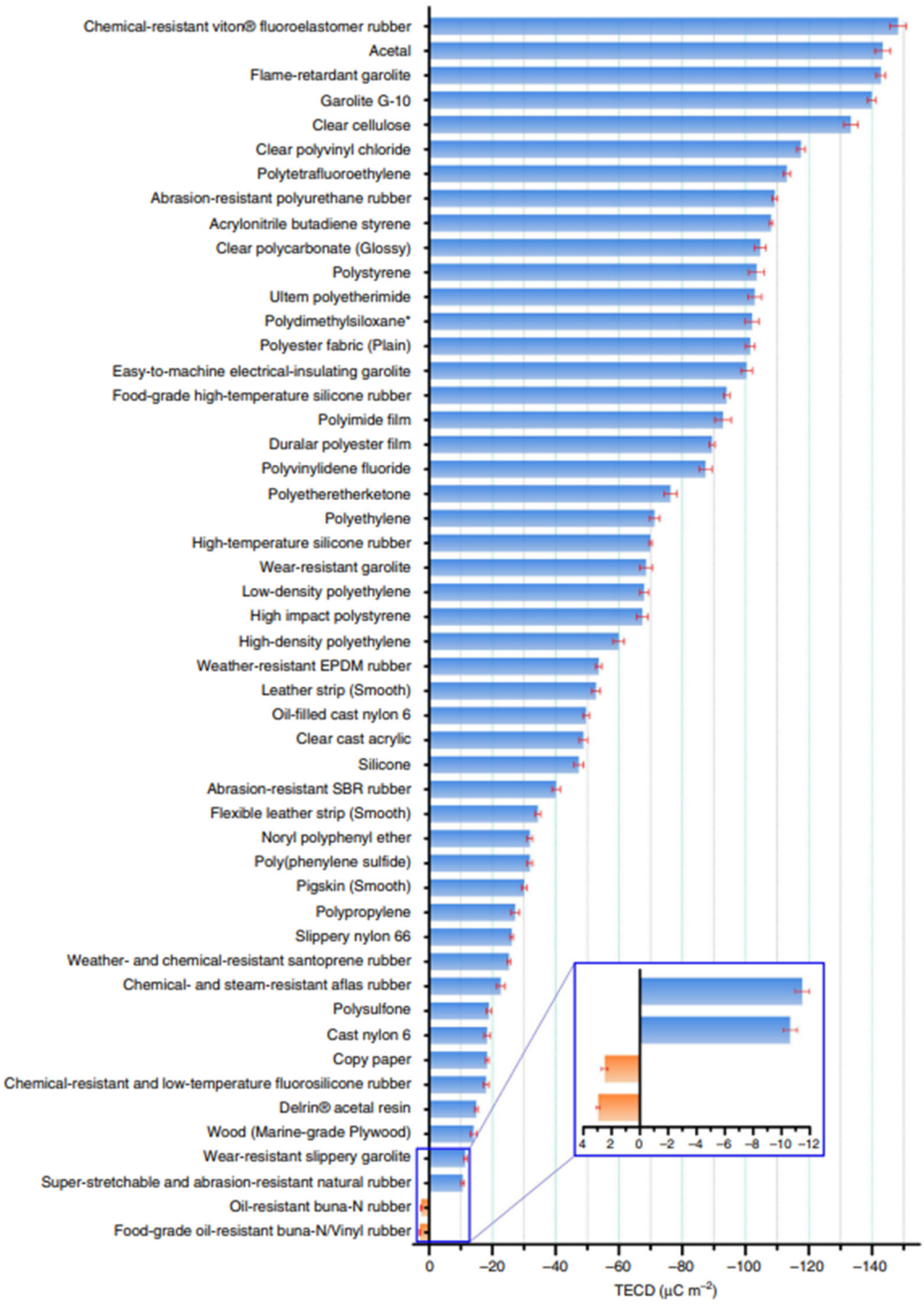

 doi:10.20944/preprints202306.0006.v1

Figure 8. The triboelectric charge density (TECD) of different triboelectric materials. Reproduced with permission from Reference [97] 2019, Nature Portfolio.

When considering the liquid phase properties of L-S TENG, two main types of liquid have been utilized: metal liquid and water. Metal liquids such as mercury and Galinstan have been chosen due to their liquid state at room temperature, excellent fluidity, and conductivity. However, their effect on TENG devices has not been studied in any paper, and they are typically used as a replacement for solid metals, acting as an electrode layer [25,100,101]. On the other hand, the properties of water carefully studied include the water forms (droplet, waves, flow), ion type, and concentration of other materials soluble in water. It is well known that the water form has a significant impact on the amount and frequency of contact between liquid and solid surfaces. With a larger contact area and higher frequency, the output power will obtain a higher result. The droplet water has been investigated to find out the effect of droplet volume, falling height, and tilting angle on L-S TENG output performance [102]. It can be seen that a droplet's volume is proportional to the velocity of the droplet. Therefore, the inertial force is affected by the droplet volume and can be expressed as $\rho v^2/D$, where ρ is density, v is velocity and D is the diameter of the droplet. However, the inertial force when the droplet moves down on the solid surface is still affected by the velocity of the droplet increases with time (ϑ_t) due to the falling height (h) and tilting angle (θ). This relationship is expressed by the Equation 1:

$$\vartheta_t = \sqrt{2gh}\, sin\theta \quad (1)$$

Due to the increment of the kinetic energy, ϑ_t increases, when falling height (h) increases, leading to an increase in the current output. Likewise, higher θ attributed to the increase of ϑ_t in Equation 1. However, the current output reaches saturation when the angle exceeds 45o and then dropped down when the inclination angle is over 75^o.

In order to achieve high output performance for energy harvesting, researchers have chosen materials with a high negative charge. Among the commonly used materials are FEP, PTFE, and PVDF, which are readily available and possess these characteristics [82,103,104]. However, the F-bonding of the hydrophobic layer when in contact with liquid will absorb the ion with low electronegativity, which decreases the TENG performance [19,32]. The high electrical conductivity ions are the reason for the low triboelectric charger on the hydrophobic layer. Besides, the adsorbed ions on the electrode layer will gradually reduce the transfer electron charge between the liquid and solid surface [105]. As shown in Figure 9a,c, the output voltage decreases when the ions concentration increase. With different types of ions (Figure 9b,d) the voltage also has different values. The results indicated that the output performance depends a lot on the properties of the ions, thereby promising that the L-S TENG device can be used for ions or chemical detection. The pH value and temperature of the water also is other affecting parameters of the TENG. The same with the ion concentration, the positive hydrogen ion (H+) increase leads to decreasing in output voltage as shown in Figure 9e [13]. As explained in the working principle, the anions causing an imbalance in the charge of liquid molecules lead to the liquid difficulty interacting with the solid surface, which is harmful to the output performance of the TENG. As shown in Figure 9f, the short-circuit current density (Jsc) decreases with increases in water temperature. The results can be explained by the change in the dielectric constant and polarity of water [43].

Preprints (www.preprints.org) | NOT PEER-REVIEWED | Posted: 1 June 2023 doi:10.20944/preprints202306.0006.v1

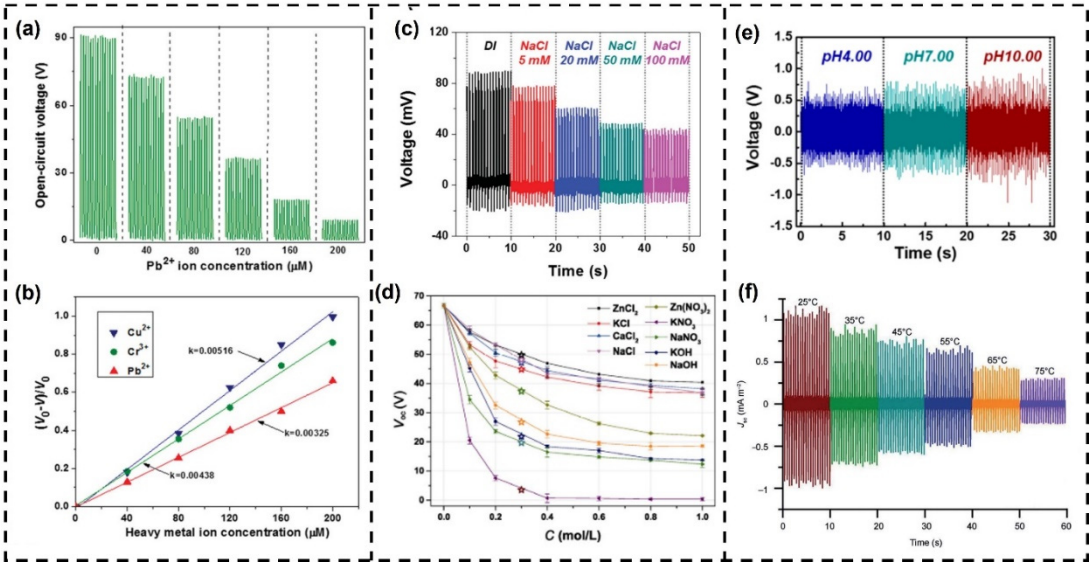

Figure 9. Performance characterization of L-S TENG in different environments. Reproduced with permission Reference [105] 2016, Wiley; and Reference [32] 2016, Wiley; Reference [105] 2016, Wiley, Reference [19] 2018, Springer Science; Reference [13] 2016, American Chemical Society; and Reference [43] 2013, Wiley.

4. L-S TENG as self-powered active pressure/touch sensors

Based on the above-mentioned operating principle of the L-S TENG, it is deduced that the variation in intensity or frequency of the dynamic fluid greatly affects the TENG electrical output; therefore, L-S TENGs can potentially appear in self-powered sensor applications in which they monitor the operations of industrial processes or detect human motions. In addition, the natural wetness of L-S TENGs contributes to decent benefits, like self-cleaning and heat-resistant properties, so that they can achieve outstanding durability and stability for long-term operation, even under severe conditions. From these aspects, among the potential applications of L-S TENG is active sensors for the monitoring of external pressure/touch in the operations of industrial processes or human motions. These triboelectric sensors with simple structures have been developed based on an L-S TENG, such as pressure, flow speed, human motions, fluctuation of a liquid surface, and so on [31,106–112].

4.1. L-S TENGs as self-powered physical sensors

It appears that L-S TENGs can offer various modes of human gesture recognition and environmental monitoring based on both the input mechanical energy and the spatial arrangement of liquid and solid materials. One example of this is a solid-liquid-solid mode TENG developed by Wang et al., which utilizes a device consisting of PTFE, water, and graphite to detect the amplitude and frequency of human fingers [113]. The water in the device not only serves as a triboelectric material but also transmits energy and signals, while the modified graphite electrode enhances the output of TENG. By tapping a finger on the PTFE sheet, this device can convert the output voltage into international Morse code using spikes and flat band signals. Two methods of Morse code encoding based on amplitude and frequency are depicted in Figure 10a, with the size and duration of signals representing "dot" and "dash". The receiving signals can be decoded in real-time on a computer screen or mobile phone.

Regarding environmental monitoring, researchers also have introduced several self-powered sensors-based L-S TENGs with remarkable performance. In particular, a self-powered water temperature sensor was proposed by Xiong et al. by applying the self-restoring, waterproof, tunable SMPU microstructural mats to fabricate the TENG with excellent superhydrophobicity (SCA = 152.2°) [114]. The self-restoring capability of the MSs mats ensures a stable triboelectric performance and a

Preprints (www.preprints.org) | NOT PEER-REVIEWED | Posted: 1 June 2023 doi:10.20944/preprints202306.0006.v1

long lifespan, even under impact and heating by hot water, thanks to the gradually increasing surface roughness during the structural recovery process triggered by water temperature. A single-electrode water-TENG design is depicted in Figure 10b, producing a series of output voltages under varying water temperatures and impacting time. Moreover, the recovery of surface roughness was recorded, and it was observed that higher temperatures could expedite the recovery process before complete recovery.

Zhang et al. built and researched a self-powered water level sensor based on LST-TENG as an example of how the L-S TENGs may be discovered in a real-time water level monitoring system (Figure 10c) [115]. The precision of the water level measurement used in this study, which is ten times greater than that of the conventional draft mark on the ship, was measured correctly and promptly for ship dynamic draft monitoring. By analyzing the peaks and valleys in the dVoc/dt signals, the water level was discovered. The peaks of the dVoc/dt signals correlate to different drafts (1, 3, 5, and 7 cm). Positive peaks in the dVoc/dt signals indicate an increase in the water level, whereas a fall in the water level results in a reduction in the dVoc/dt value. Such a phenomenon is brought on by the fact that the Voc increases/decreases more quickly as the water rises/falls in the electrode region while doing so more slowly in the blank region.

Other than the above-mentioned functions, by combining liquid-solid contact-electrification with the Venturi tube structure, a Venturi-type triboelectric flow sensor (VTTFS) was fabricated [116]. The experimental flow measuring system is shown in Figure 10d. The results show that when the flow is progressively increased from 95 L/min to 215 L/min, the overall trend is rising, and when the flow is gradually decreased, the overall trend is declining. The matching pulse counts exhibit a superb linear connection with the varying flow. The VTTFS was also evaluated in irregular flow conditions, and the electrical pulse signal generated shows a one-to-one relationship to the flow. The industrial production industry, pipeline transportation, measurement research, and even medical healthcare equipment are all potential markets for this flow-sensing method.

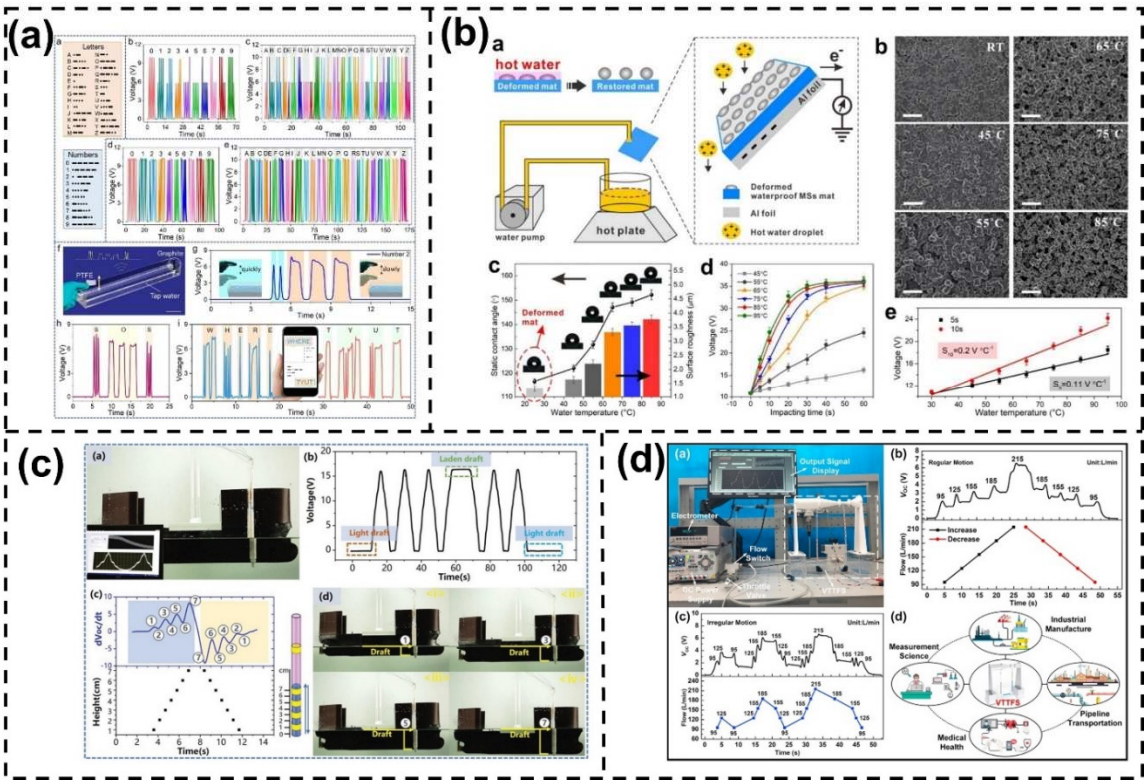

Figure 10. (a) Electrical response from the TENG and self-powered communication a solid-liquid-solid interaction; (b) Electrospun MSs mat-based water-TENG for self-powered water temperature sensor; (c) The application of LST-TENG as a water level sensor for ship draft detecting; (d) Flow and level sensing by waveform coupled liquid-solid contact-electrification. Reproduced with permission

Preprints (www.preprints.org) | NOT PEER-REVIEWED | Posted: 1 June 2023 doi:10.20944/preprints202306.0006.v1

Reference [113] 2022, Elsevier; Reference [114] 2019, Elsevier; Reference [115] 2019, Wiley; Reference [116] 2021, Elsevier.

4.2. L-S TENGs as self-powered pressure/force sensors

Pressure sensors are developing rapidly across the world with a variety of applications like a healthcare monitoring system [108,109], game control, and soft robotics [110,117]. In numerous real-world situations, pressure sensors must operate with a basic model or without a power source. Therefore, developing these systems to be the smallest, wireless, and maintenance-free is made possible by self-powered sensor-based triboelectrification. Pressure sensors based L-S TENG have a straightforward design and are economical for detecting in vast regions and low-temperature conditions [111].

To develop the L-S TENG-based pressure sensor, several device structures have been designed. For example, a highly flexible microfluidic channel based on TENG has been demonstrated by some researchers [111,112,118], and a simple U-tube based on TENG has also shown good results for pressure sensing [20,107]. The U-shaped TENG fabrications from common materials in the industry and daily life have been explored based on Pascal's law in order to gain a deeper quantitative grasp of the L-S TENG-based pressure sensor. Figure 11a illustrates the testing configuration for the U-shaped TENG as dynamic pressure sensing using a tube constructed of FEP with an inner diameter of 20 mm [20]. When pressure is applied to the U-tube, the largest height difference between the two column fluid levels is ΔH. The acceleration (a), with respect to a constant vibration frequency, is completely dictated by the vibration amplitudes (x), and the transferred charge can be calculated by equation 2:

$$Q_{SC} = 2\pi\sigma r\Delta H \quad (2)$$

Where σ is the surface tribo-charges density, r is the diameter of the tube. From this equation, the short-circuit current at t is the time given by:

$$I_{SC} = 2\pi\sigma r\frac{d\Delta H}{dt} = 2\pi\sigma rV(t) \quad (3)$$

Where V(t) is the water flow rate. As can be seem, short-circuit current (ISC) is proportional to V(t) and ΔH. Here, the applied pressure (P) into the U-tube can be represented by the height difference in liquid level, so the measured output performance is proportional to the pressure. As shown in Figure 11c,f, the relationship of open-circuit voltages and short-circuit current with pressure displayed good linear behavior ($R^2 = 0.998$) at a low-pressure regime (from 0.16 kPa to 0.54 kPa). The result has shown that detailed information about the ambient mechanical motions can be monitored by the TENG device when combining the analysis of both the Voc and Isc measurements. Moreover, using a microfluidic channel design can shrink down the repeated system and achieve higher output performance compared to a U-tube structure. Due to its advantages of being battery-free, having a straightforward operating mechanism, and being inexpensive, self-powered sensors can be used in blood pressure monitoring, pulse waveform monitoring, electronic skin, and other applications.

Preprints (www.preprints.org) | NOT PEER-REVIEWED | Posted: 1 June 2023 doi:10.20944/preprints202306.0006.v1

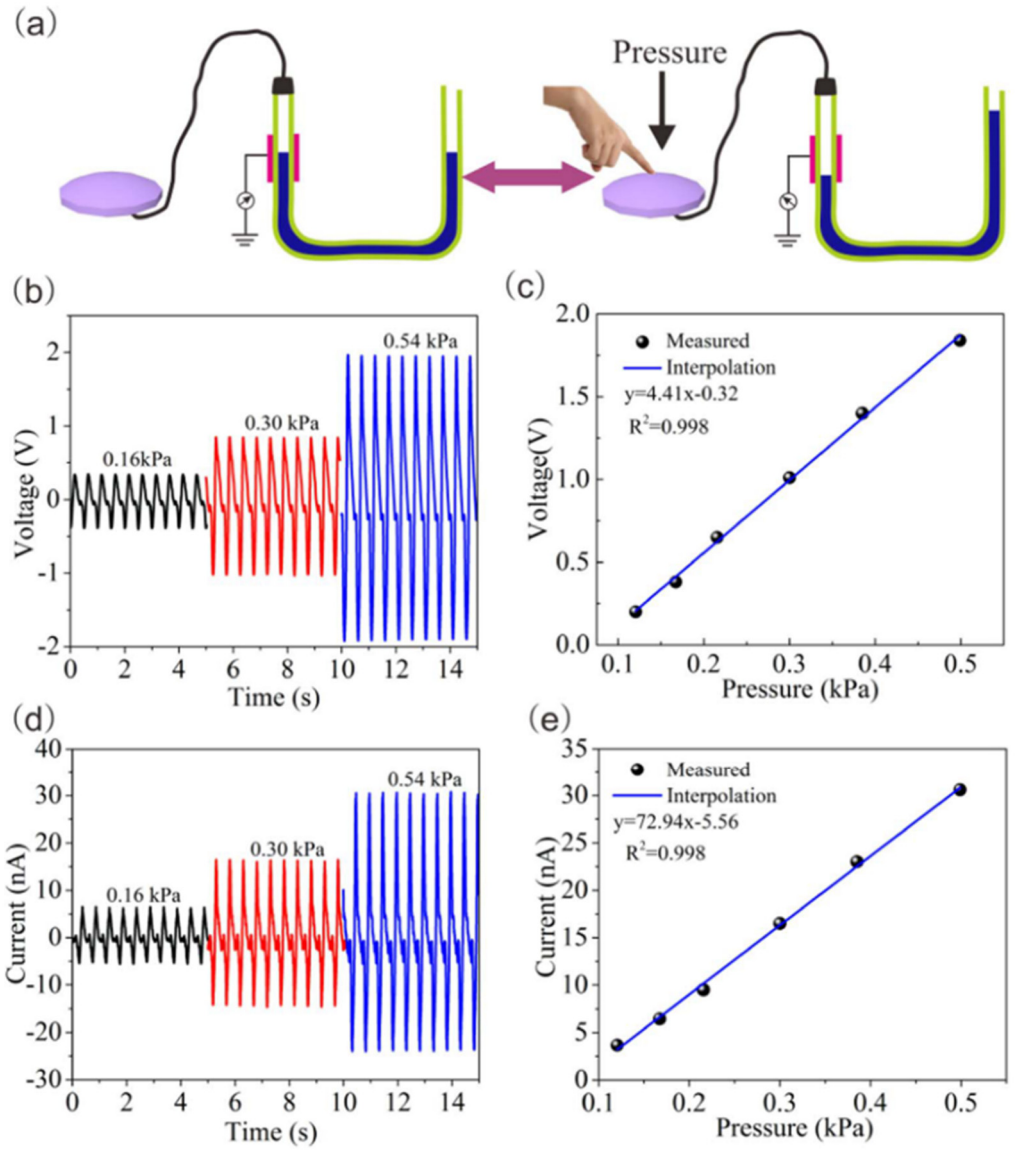

Figure 11. (a) Testing setup for U-shaped TENG as dynamic pressure sensing, (b) The open-circuit voltage peak at different pressure and (c) its relationship, (d) The short-circuit current peak at different pressure, and (e) its relationship Reproduced with permission Reference [20] 2017, Elsevier.

5. L-S TENGs as self-powered chemical/environment sensors

Chemical detection and environmental factor sensing are crucial for maintaining the quality of water or wastewater. The self-powered sensor of the change of the liquid characteristics development may use the influence of the liquid phase on L-S TENG [19]. As the proportionate to the triboelectric charge density varied, the produced electrical signal in an L-S TENG would have fluctuated. Assuming all other factors remain constant, the chemical characteristics of the liquid may affect how the charge is absorbed by the solid surface, changing the triboelectric charge density. We have attempted to categorize the group of self-powered sensors in this part using various liquid properties e.g. ion liquid concentration [13,119], organic concentration [89,120], chemical detection [121], biological response [35,43].

Figure 12a shows the average output voltage values generated by various NaCl solution concentrations from 0 to 0.75 M.32 When the NaCl concentration rose from 0.005 to 0.1M, it would have appeared that the voltage output of the L-S TENG dropped quickly. Various other studies represent the same result about the harmful of different ionic compounds (such as $ZnCl_2$, KCl, $CaCl_2$, KNO_3, $NaNO_3$, KOH, NaOH, and so on) on the output performance [13,19,70,122]. Moreover, based

Preprints (www.preprints.org) | NOT PEER-REVIEWED | Posted: 1 June 2023 doi:10.20944/preprints202306.0006.v1

on the electronegativity properties of the cation or anion, the decline of the voltage shows a significant difference. The sensitivity of the self-powered TENG sensor with NaCl concentrations ranging from 0 M to 0.75 M is shown in Figure 12b. The output voltage ratio (ΔV/V) and the concentration of NaCl have a linear relationship, and the sensor exhibits great sensitivity in the range of 0.005 M to 0.1 M. The outcome supports the possibility of using L-S TENG in a self-powered sensor with very low ion liquid concentration. Moreover, Figure 12c,d illustrates the sensor's stated selectivity [105]. Several modifying agents can be used to alter the output voltage ratio of each ion liquid under the same testing conditions. A TENG sensor was modified with dithizone to enable the detection of Pb2+, and the results demonstrate that additional heavy metal ions have bigger output voltage ratios. When diphenylcarbazide is used as the modifying agent, the outcome is the same as Cr3+. It is clear that self-powered L-S TENG sensors offer excellent selectivity and sensitivity for measuring ions concentration.

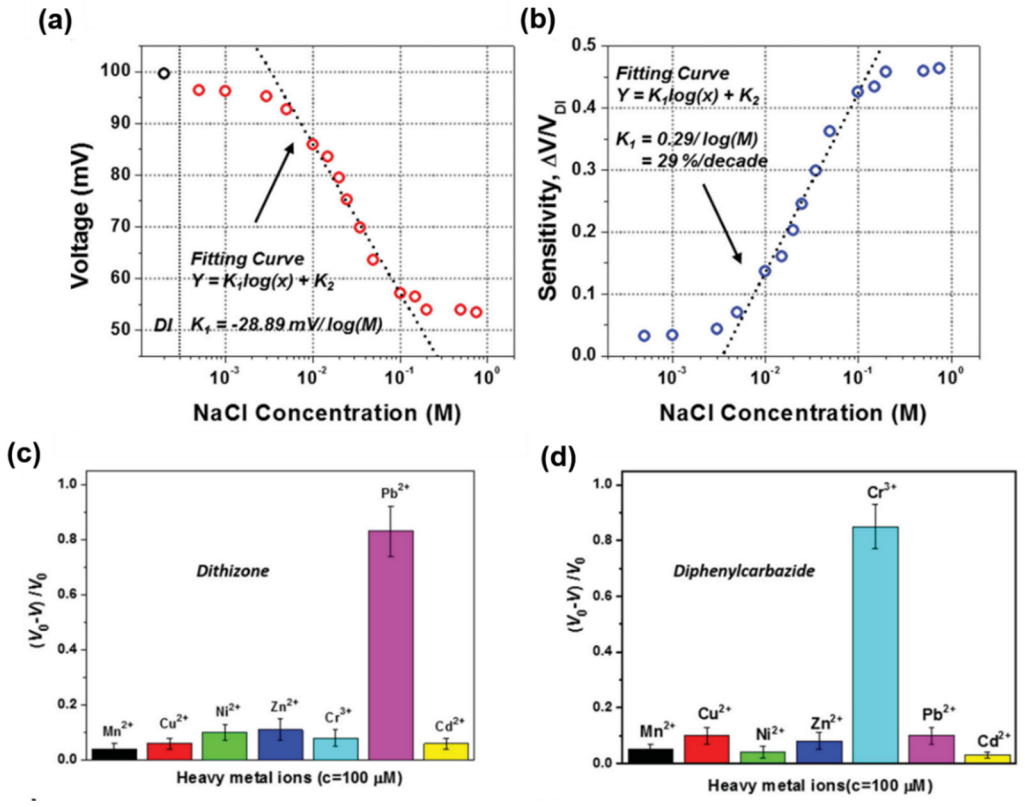

Figure 12. (a) Average output voltage values generated by various NaCl solution concentration from 0 to 0.75 M and (b) the sensitivity of the sensor during its NaCl solution concentration; A test of selectivity of the self-powered triboelectric sensor for (c) Pb2+ detection by using dithizone and as the surface modifying agent (d) Cr3+ detection by using diphenylcarbazide as the surface modifying agent. Reproduced with permission Reference [32] 2016, Wiley; Reference [105] 2016, Wiley.

Fermentation, biomedicine, and other chemical activities all heavily rely on organic liquids and gases. As a result, monitoring and managing the organic concentration is essential for optimizing industrial operations and raising the quality of life. For the detection of ethanol, formaldehyde, and glucose, a self-powered sensor based on a triboelectric nanogenerator device has recently gained a lot of interest [89,120]. A self-powered TENG sensor design for organic concentration based on industry-standard PTFE filtering membranes is depicted in Figure 13a. Positive water charges will build up on the surface side that is in touch with the liquid and PTFE when the water is propelled by external mechanical vibration. An alternating current is produced by the water repeatedly contacting and separating from the PTFE surface. The current of the TENG substantially reduces when an organic liquid with increasing concentration is used to replace water. It can appear that the formaldehyde and ethanol concentrations are measured using the TENG instrument.

Preprints (www.preprints.org) | NOT PEER-REVIEWED | Posted: 1 June 2023 doi:10.20944/preprints202306.0006.v1

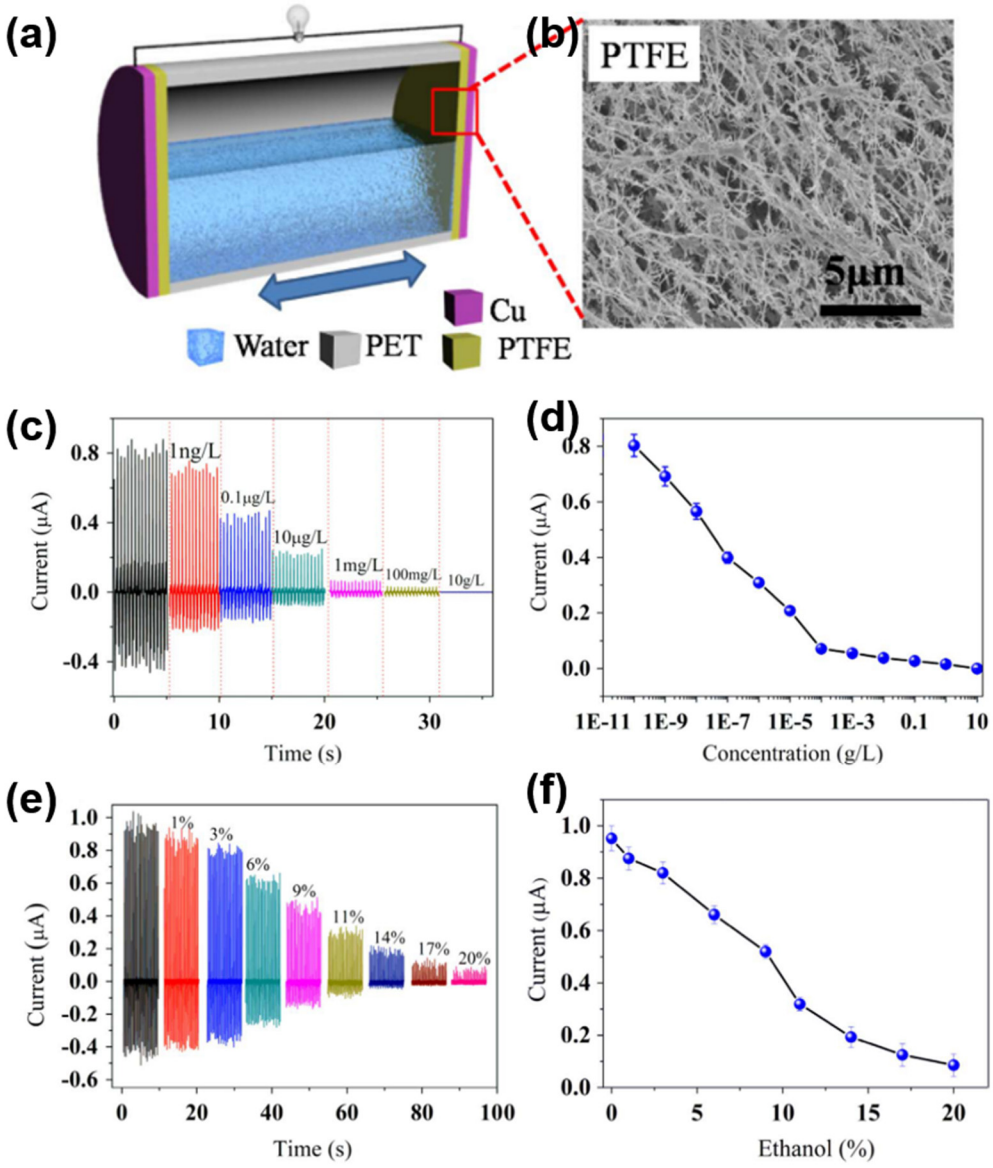

Figure 13. (a) Schematic illustration of the self-powered TENG sensor for organic concentration and (b) the FESEM image of PTFE membranes surface; (c, d) Short-circuit current for different formaldehyde concentrations and (e, f) Short-circuit current for different ethanol concentrations (percentage by volume). Reproduced with permission Reference [49] 2016, Elsevier.

In addition to an application for self-powered sensors, chemical sensing has been developed in recent years, owing to life safety and industrial processes control. Figure 14a,c show the working mechanism of a single electrode L-S TENG (SELS-TENG) and contact-separation L-S TENG (CSLS-TENG) based sensor [121,123]. The working mechanism is also the same and has been explained in the working principal section. Based on different chemicals, the output signal shows a different result. In Figure 14b, the current of the SLES-TENG showed a positive peak and the value mainly around 100nA for alcohol 99.7% detection. On the contrary, for acetone 99.5% sense, the current has a negative peak and the value has dropped to -80 nA. Moreover, the current to sensing NaOH and NaCl also shows the difference when the current value is around +200 nA and -250 nA. In summary, the varied ions present in the liquid have an impact on the output current. The voltage and current of the self-powered sensor-based TENG are shown in excellent detail in Figure 14d. It is clear that the

Preprints (www.preprints.org) | NOT PEER-REVIEWED | Posted: 1 June 2023 doi:10.20944/preprints202306.0006.v1

voltage and current characteristics or values will affect the detection and classification of different liquids.

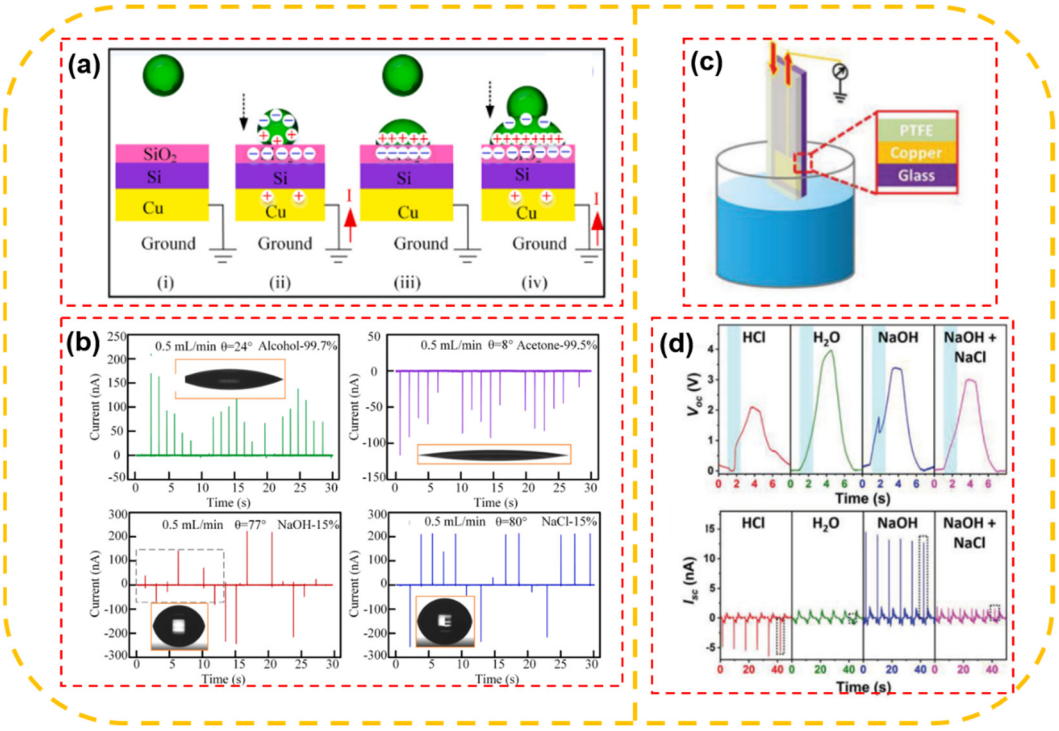

Figure 14. (a) The working mechanism of L-S TENG-based sensor and (b) Isc with different liquid alcohol, acetone, NaOH liquid, NaCl liquid; (c) Schematic illustration of the L-S TENG and (d) Voc and Isc in paraffin oil/water with different aqueous solutions of HCl (0.1 mol.L−1), deionized water, NaOH (0.1 mol.L−1), and mixture solution of NaOH and NaCl (0.1 mol.L−1). Reproduced with permission Reference [121] 2019, Elsevier; Reference [123] 2019, Wiley.

6. Conclusion

Sensors have become an integral component of modern technology, enabling devices and systems to detect and respond to signals from the environment, humans, animals, and other sources. In order to power these devices without using external power sources, self-powered sensors have emerged as a possible approach. The potential for creating sophisticated sensing systems has increased with the rise of L-S TENG as a significant technology in the field of self-powered sensors. One of the main benefits of L-S TENG is its capacity to produce electricity from a variety of mechanical stimuli. This makes it suitable for use in a variety of sensing applications, including pressure sensing, touch detection, flow rate monitoring, and chemical and biological detection. The device is also highly efficient at converting mechanical energy into electrical energy, making it an attractive option for powering small electronic devices. Another advantage of L-S TENG is its low cost and environmental friendliness. The device can be fabricated using simple and inexpensive materials, making it accessible to a wide range of users. Additionally, the device does not rely on external power sources, reducing the environmental impact associated with battery disposal and replacement.

Despite its many advantages, there are still challenges associated with the use of L-S TENG for sensing applications. One of the main challenges is the need to optimize the device for specific applications, as the performance of the device can vary depending on the materials and design used. Additionally, the device may be susceptible to wear and tear over time, which can reduce its efficiency and longevity.

Despite these challenges, the development of self-powered sensors based on L-S TENG is a significant step forward in the field of sensing technology. With their low cost, high stability, and ability to generate electricity from mechanical stimuli, these sensors have the potential to

revolutionize a wide range of industries and applications, from healthcare and biomedicine to environmental monitoring and industrial automation. As research in this field continues to advance, it is likely that we will see new and innovative applications of L-S TENG-based sensors in the years to come.

Author Contributions: Conceptualization, Q.T.N.; validation C.D.L.; investigation, Q.T.N. and D.L.V.; resources, D.L.V.; writing—original draft preparation, Q.T.N., D.L.V. and C.D.L.; writing—review and editing, C.D.L. and D.L.V.; visualization, Q.T.N.; supervision, K.K.A.; project administration, K.K.A.; funding acquisition, K.K.A. All authors have read and agreed to the published version of the manuscript.

Funding: This research was supported by Basic Science Research Program through the National Research Foundation of Korea (NRF) funded by the Ministry of Science and ICT, South Korea (NRF-2020R1A2B5B03001480) and by "Regional Innovation Strategy (RIS)" through the National Research Foundation of Korea(NRF) funded by the Ministry of Education(MOE)(2021RIS-003).

Institutional Review Board Statement: Not applicable.

Informed Consent Statement: Not applicable.

Data Availability Statement: Not applicable.

Conflicts of Interest: The authors declare no conflict of interest.

References

1. Cai G, Liang Y, Liu Z, Liu W. Design and optimization of bio-inspired wave-like channel for a PEM fuel cell applying genetic algorithm. Energy. 2020;192.
2. Muetze A, Vining JG. Ocean Wave Energy Conversion - A Survey. Conference Record of the 2006 IEEE Industry Applications Conference Forty-First IAS Annual Meeting2006. p. 1410-7.
3. Sabzehgar R, Moallem M. A review of ocean wave energy conversion systems. 2009 IEEE Electrical Power & Energy Conference (EPEC)2009. p. 1-6.
4. Chang C, Tran VH, Wang J, Fuh Y-K, Lin L. Direct-write piezoelectric polymeric nanogenerator with high energy conversion efficiency. Nano Lett. 2010;10(2):726-31.
5. Zhang C, Tang W, Han C, Fan F, Wang ZL. Theoretical comparison, equivalent transformation, and conjunction operations of electromagnetic induction generator and triboelectric nanogenerator for harvesting mechanical energy. Adv Mater. 2014;26(22):3580-91.
6. Wang X, Song J, Liu J, Wang ZL. Direct-current nanogenerator driven by ultrasonic waves. Science. 2007;316(5821):102-5.
7. Wang ZL, Jun LL, Simiao C, Zi NY. Triboelectric Nanogenerators2016.
8. Jiang D, Xu M, Dong M, Guo F, Liu X, Chen G, et al. Water-solid triboelectric nanogenerators: An alternative means for harvesting hydropower. Renew Sustain Energy Rev. 2019;115.
9. Wang ZL, Jiang T, Xu L. Toward the blue energy dream by triboelectric nanogenerator networks. Nano Energy. 2017;39:9-23.
10. Bai P, Zhu G, Lin Z-H, Jing Q, Chen J, Zhang G, et al. Integrated multilayered triboelectric nanogenerator for harvesting biomechanical energy from human motions. ACS Nano. 2013;7(4):3713-9.
11. Wang ZL, Chen J, Lin L. Progress in triboelectric nanogenerators as a new energy technology and self-powered sensors. Energy Environ Sci. 2015;8(8):2250-82.
12. Fan F-R, Tian Z-Q, Lin Wang Z. Flexible triboelectric generator. Nano Energy. 2012;1(2):328-34.
13. Lee S, Chung J, Kim DY, Jung JY, Lee SH, Lee S. Cylindrical water triboelectric nanogenerator via controlling geometrical shape of anodized aluminum for enhanced electrostatic induction. ACS Appl Mater Interfaces. 2016;8(38):25014-8.
14. Zhu G, Lin ZH, Jing Q, Bai P, Pan C, Yang Y, et al. Toward large-scale energy harvesting by a nanoparticle-enhanced triboelectric nanogenerator. Nano Lett. 2013;13(2):847-53.
15. Lin ZH, Cheng G, Lee S, Pradel KC, Wang ZL. Harvesting water drop energy by a sequential contact-electrification and electrostatic-induction process. Adv Mater. 2014;26(27):4690-6.
16. Wang Y, Yang Y, Wang ZL. Triboelectric nanogenerators as flexible power sources. npj Flex Electron. 2017;1(1).
17. Cheedarala RK, Duy LC, Ahn KK. Double characteristic BNO-SPI-TENGs for robust contact electrification by vertical contact separation mode through ion and electron charge transfer. Nano Energy. 2018;44:430-7.
18. Shi Q, He T, Lee C. More than energy harvesting – Combining triboelectric nanogenerator and flexible electronics technology for enabling novel micro-/nano-systems. Nano Energy. 2019;57:851-71.
19. Pan L, Wang J, Wang P, Gao R, Wang Y-C, Zhang X, et al. Liquid-FEP-based U-tube triboelectric nanogenerator for harvesting water-wave energy. Nano Res. 2018;11(8):4062-73.

20. Zhang X, Zheng Y, Wang D, Zhou F. Solid-liquid triboelectrification in smart U-tube for multifunctional sensors. Nano Energy. 2017;40:95-106.
21. Seol M-L, Jeon S-B, Han J-W, Choi Y-K. Ferrofluid-based triboelectric-electromagnetic hybrid generator for sensitive and sustainable vibration energy harvesting. Nano Energy. 2017;31:233-8.
22. Zhao XJ, Tian JJ, Kuang SY, Ouyang H, Yan L, Wang ZL, et al. Biocide-free antifouling on insulating surface by wave-driven triboelectrification-induced potential oscillation. Adv Mater Interfaces. 2016;3(17):1600187.
23. Vu DL, Ahn KK. Triboelectric enhancement of polyvinylidene fluoride membrane using magnetic nanoparticle for water-based energy harvesting. Polymers (Basel). 2022;14(8):1547.
24. Le C-D, Vo C-P, Nguyen T-H, Vu D-L, Ahn KK. Liquid-solid contact electrification based on discontinuous-conduction triboelectric nanogenerator induced by radially symmetrical structure. Nano Energy. 2021;80:105571.
25. Tang W, Jiang T, Fan FR, Yu AF, Zhang C, Cao X, et al. Liquid-Metal Electrode for High-Performance Triboelectric Nanogenerator at an Instantaneous Energy Conversion Efficiency of 70.6%. Adv Funct Mater. 2015;25(24):3718-25.
26. Zhao XJ, Zhu G, Fan YJ, Li HY, Wang ZL. Triboelectric Charging at the Nanostructured Solid/Liquid Interface for Area-Scalable Wave Energy Conversion and Its Use in Corrosion Protection. Acs Nano. 2015;9(7):7671-7.
27. Cheedarala RK, Shahriar M, Ahn JH, Hwang JY, Ahn KK. Harvesting liquid stream energy from unsteady peristaltic flow induced pulsatile Flow-TENG (PF-TENG) using slipping polymeric surface inside elastomeric tubing. Nano Energy. 2019;65.
28. Wang ZL. Triboelectric nanogenerators as new energy technology and self-powered sensors - principles, problems and perspectives. Faraday Discuss. 2014;176:447-58.
29. Kwon S-H, Park J, Kim WK, Yang Y, Lee E, Han CJ, et al. An effective energy harvesting method from a natural water motion active transducer. Energy Environ Sci. 2014;7(10):3279-83.
30. Cheng G, Lin Z-H, Du Z-l, Wang ZL. Simultaneously Harvesting Electrostatic and Mechanical Energies from Flowing Water by a Hybridized Triboelectric Nanogenerator. ACS Nano. 2014;8(2):1932-9.
31. Zhang L, Zhang N, Yang Y, Xiang S, Tao C, Yang S, et al. Self-powered all-in-one fluid sensor textile with enhanced triboelectric effect on all-immersed dendritic liquid-solid interface. ACS Appl Mater Interfaces. 2018;10(36):30819-26.
32. Jeon S-B, Seol M-L, Kim D, Park S-J, Choi Y-K. Self-powered ion concentration sensor with triboelectricity from liquid-solid contact electrification. Adv Electron Mater. 2016;2(5):1600006.
33. Xu M, Wang S, Zhang SL, Ding W, Kien PT, Wang C, et al. A highly-sensitive wave sensor based on liquid-solid interfacing triboelectric nanogenerator for smart marine equipment. Nano Energy. 2019;57:574-80.
34. Kim W, Choi D, Kwon J-Y, Choi D. A self-powered triboelectric microfluidic system for liquid sensing. J Mate Chem A. 2018;6(29):14069-76.
35. Yi F, Wang X, Niu S, Li S, Yin Y, Dai K, et al. A highly shape-adaptive, stretchable design based on conductive liquid for energy harvesting and self-powered biomechanical monitoring. Sci Adv. 2016;2(6):e1501624.
36. Cui S, Zheng Y, Zhang T, Wang D, Zhou F, Liu W. Self-powered ammonia nanosensor based on the integration of the gas sensor and triboelectric nanogenerator. Nano Energy. 2018;49:31-9.
37. Wang H, Wu H, Hasan D, He T, Shi Q, Lee C. Self-powered dual-mode amenity sensor based on the water-air triboelectric nanogenerator. ACS Nano. 2017;11(10):10337-46.
38. Zhou L, Liu D, Wang J, Wang ZL. Triboelectric nanogenerators: Fundamental physics and potential applications. Friction. 2020;8(3):481-506.
39. Wang ZL, Wang AC. On the origin of contact-electrification. Mater Today. 2019;30:34-51.
40. Lin S, Chen X, Wang ZL. Contact Electrification at the Liquid–Solid Interface. Chemical Reviews. 2021;122(5):5209-32.
41. Lin S, Xu L, Chi Wang A, Wang ZL. Quantifying electron-transfer in liquid-solid contact electrification and the formation of electric double-layer. Nat Commun. 2020;11(1):399.
42. Nie J, Ren Z, Xu L, Lin S, Zhan F, Chen X, et al. Probing Contact-Electrification-Induced Electron and Ion Transfers at a Liquid-Solid Interface. Adv Mater. 2020;32(2):e1905696.
43. Lin ZH, Cheng G, Lin L, Lee S, Wang ZL. Water-solid surface contact electrification and its use for harvesting liquid-wave energy. Angew Chem Int Ed Engl. 2013;52(48):12545-9.
44. Kim T, Kim DY, Yun J, Kim B, Lee SH, Kim D, et al. Direct-current triboelectric nanogenerator via water electrification and phase control. Nano Energy. 2018;52:95-104.
45. Lee JH, Kim S, Kim TY, Khan U, Kim S-W. Water droplet-driven triboelectric nanogenerator with superhydrophobic surfaces. Nano Energy. 2019;58:579-84.
46. Yang X, Chan S, Wang L, Daoud WA. Water tank triboelectric nanogenerator for efficient harvesting of water wave energy over a broad frequency range. Nano Energy. 2018;44:388-98.
47. Lee J-W, Hwang W. Theoretical study of micro/nano roughness effect on water-solid triboelectrification with experimental approach. Nano Energy. 2018;52:315-22.

48. Nahian SA, Cheedarala RK, Ahn KK. A study of sustainable green current generated by the fluid-based triboelectric nanogenerator (FluTENG) with a comparison of contact and sliding mode. Nano Energy. 2017;38:447-56.
49. Zhang X, Zheng Y, Wang D, Rahman ZU, Zhou F. Liquid–solid contact triboelectrification and its use in self-powered nanosensor for detecting organics in water. Nano Energy. 2016;30:321-9.
50. Huang T, Hao X, Li M, He B, Sun W, Zhang K, et al. A Multifunction Freestanding Liquid-Solid Triboelectric Nanogenerator Based on Low-Frequency Mechanical Sloshing. ACS Appl Mater Interfaces. 2022;14(49):54716-24.
51. Guang Zhu YS, Peng Bai, Jun Chen, Qingshen Jing, Weiqing Yang, and Zhong Lin Wang. Harvesting Water Wave Energy by Asymmetric Screening of Electrostatic Charges on a Nanostructured Hydrophobic Thin-Film Surface. ACS Nano. 2014;8(6):6031-7.
52. Zhao XJ, Kuang SY, Wang ZL, Zhu G. Highly adaptive solid-liquid interfacing triboelectric nanogenerator for harvesting diverse water wave energy. ACS Nano. 2018;12(5):4280-5.
53. Choi D, Kim DW, Yoo D, Cha KJ, La M, Kim DS. Spontaneous occurrence of liquid-solid contact electrification in nature: Toward a robust triboelectric nanogenerator inspired by the natural lotus leaf. Nano Energy. 2017;36:250-9.
54. Jang S, La M, Cho S, Yun Y, Choi JH, Ra Y, et al. Monocharged electret based liquid-solid interacting triboelectric nanogenerator for its boosted electrical output performance. Nano Energy. 2020;70.
55. Kil Yun B, Soo Kim H, Joon Ko Y, Murillo G, Hoon Jung J. Interdigital electrode based triboelectric nanogenerator for effective energy harvesting from water. Nano Energy. 2017;36:233-40.
56. Kim T, Chung J, Kim DY, Moon JH, Lee S, Cho M, et al. Design and optimization of rotating triboelectric nanogenerator by water electrification and inertia. Nano Energy. 2016;27:340-51.
57. Le C-D, Vo C-P, Nguyen T-H, Vu D-L, Ahn KK. Liquid-solid contact electrification based on discontinuous-conduction triboelectric nanogenerator induced by radially symmetrical structure. Nano Energy. 2021;80.
58. Li C, Liu X, Yang D, Liu Z. Triboelectric nanogenerator based on a moving bubble in liquid for mechanical energy harvesting and water level monitoring. Nano Energy. 2022;95.
59. Liu L, Shi Q, Ho JS, Lee C. Study of thin film blue energy harvester based on triboelectric nanogenerator and seashore IoT applications. Nano Energy. 2019;66.
60. Yoo D, Park S-C, Lee S, Sim J-Y, Song I, Choi D, et al. Biomimetic anti-reflective triboelectric nanogenerator for concurrent harvesting of solar and raindrop energies. Nano Energy. 2019;57:424-31.
61. Yu J, Ma T. Triboelectricity-based self-charging droplet capacitor for harvesting low-level ambient energy. Nano Energy. 2020;74.
62. Choi D, Lee S, Park SM, Cho H, Hwang W, Kim DS. Energy harvesting model of moving water inside a tubular system and its application of a stick-type compact triboelectric nanogenerator. Nano Research. 2015;8(8):2481-91.
63. Lu Y, Yan Y, Yu X, Zhou X, Feng S, Xu C, et al. Polarized Water Driven Dynamic PN Junction-Based Direct-Current Generator. Research (Wash D C). 2021;2021:7505638.
64. Zhang J, Lin S, Zheng M, Wang ZL. Triboelectric Nanogenerator as a Probe for Measuring the Charge Transfer between Liquid and Solid Surfaces. ACS Nano. 2021;15(9):14830-7.
65. Li X, Tao J, Wang X, Zhu J, Pan C, Wang ZL. Networks of High Performance Triboelectric Nanogenerators Based on Liquid-Solid Interface Contact Electrification for Harvesting Low-Frequency Blue Energy. Adv Energy Mater. 2018;8(21).
66. Yang L, Wang Y, Guo Y, Zhang W, Zhao Z. Robust Working Mechanism of Water Droplet-Driven Triboelectric Nanogenerator: Triboelectric Output versus Dynamic Motion of Water Droplet. Adv Mater Interfaces. 2019;6(24).
67. Nguyen QT, Vo CP, Nguyen TH, Ahn KK. A Direct-Current Triboelectric Nanogenerator Energy Harvesting System Based on Water Electrification for Self-Powered Electronics. Applied Sciences. 2022;12(5).
68. Wang L, Song Y, Xu W, Li W, Jin Y, Gao S, et al. Harvesting energy from high-frequency impinging water droplets by a droplet-based electricity generator. EcoMat. 2021;3(4).
69. Helseth LE. Electrical energy harvesting from water droplets passing a hydrophobic polymer with a metal film on its back side. Journal of Electrostatics. 2016;81:64-70.
70. Park H-Y, Kim HK, Hwang Y-H, Shin D-M. Water-through triboelectric nanogenerator based on Ti-mesh for harvesting liquid flow. J Korean Phys Soc. 2018;72(4):499-503.
71. Cho H, Chung J, Shin G, Sim J-Y, Kim DS, Lee S, et al. Toward sustainable output generation of liquid–solid contact triboelectric nanogenerators: The role of hierarchical structures. Nano Energy. 2019;56:56-64.
72. Li Z, Yang D, Zhang Z, Lin S, Cao B, Wang L, et al. A droplet-based electricity generator for large-scale raindrop energy harvesting. Nano Energy. 2022;100.
73. Munirathinam K, Kim D-S, Shanmugasundaram A, Park J, Jeong Y-J, Lee D-W. Flowing water-based tubular triboelectric nanogenerators for sustainable green energy harvesting. Nano Energy. 2022;102.

74. Kwak SS, Lin S, Lee JH, Ryu H, Kim TY, Zhong H, et al. Triboelectrification-Induced Large Electric Power Generation from a Single Moving Droplet on Graphene/Polytetrafluoroethylene. ACS Nano. 2016;10(8):7297-302.
75. Yan Y, Zhou X, Feng S, Lu Y, Qian J, Zhang P, et al. Direct Current Electricity Generation from Dynamic Polarized Water–Semiconductor Interface. The Journal of Physical Chemistry C. 2021;125(26):14180-7.
76. Dong J, Xu C, Zhu L, Zhao X, Zhou H, Liu H, et al. A high voltage direct current droplet-based electricity generator inspired by thunderbolts. Nano Energy. 2021;90.
77. Helseth LE. A water droplet-powered sensor based on charge transfer to a flow-through front surface electrode. Nano Energy. 2020;73.
78. Li X, Ning X, Li L, Wang X, Li B, Li J, et al. Performance and power management of droplets-based electricity generators. Nano Energy. 2022;92.
79. Wijewardhana KR, Shen T-Z, Jayaweera EN, Shahzad A, Song J-K. Hybrid nanogenerator and enhancement of water–solid contact electrification using triboelectric charge supplier. Nano Energy. 2018;52:402-7.
80. Xu W, Zheng H, Liu Y, Zhou X, Zhang C, Song Y, et al. A droplet-based electricity generator with high instantaneous power density. Nature. 2020;578(7795):392-6.
81. Sun W, Zheng Y, Li T, Feng M, Cui S, Liu Y, et al. Liquid-solid triboelectric nanogenerators array and its applications for wave energy harvesting and self-powered cathodic protection. Energy. 2021;217.
82. Liu Y, Zheng Y, Li T, Wang D, Zhou F. Water-solid triboelectrification with self-repairable surfaces for water-flow energy harvesting. Nano Energy. 2019;61:454-61.
83. Tan J, Duan J, Zhao Y, He B, Tang Q. Generators to harvest ocean wave energy through electrokinetic principle. Nano Energy. 2018;48:128-33.
84. Yang Dong SX, Chi Zhang, Liqiang Zhang, Daoai Wang,, Yuanyuan Xie NL, Yange Feng, Nannan Wang, Min Feng, Xiaolong Zhang,, Feng Zhou ZLW. Gas-liquid two-phase flow-based triboelectric nanogenerator with ultrahigh output power. Science advances. 2022;8.
85. Vu DL, Le CD, Ahn KK. Functionalized graphene oxide/polyvinylidene fluoride composite membrane acting as a triboelectric layer for hydropower energy harvesting. Int J Energy Res. 2022:9549- 59.
86. Vu DL, Ahn KK. High-Performance Liquid-Solid Triboelectric Nanogenerator Based on Polyvinylidene Fluoride and Magnetic Nanoparticle Composites Film. 2021 24th International Conference on Mechatronics Technology (ICMT)2021. p. 1-5.
87. Vu DL, Le CD, Vo CP, Ahn KK. Surface polarity tuning through epitaxial growth on polyvinylidene fluoride membranes for enhanced performance of liquid-solid triboelectric nanogenerator. Compos Pt B-Eng. 2021;223:109135.
88. Helseth LE, Guo XD. Contact electrification and energy harvesting using periodically contacted and squeezed water droplets. Langmuir. 2015;31(10):3269-76.
89. Lin ZH, Cheng G, Wu WZ, Pradel KC, Wang ZL. Dual-Mode Triboelectric Nanogenerator for Harvesting Water Energy and as a Self-Powered Ethanol Nanosensor. Acs Nano. 2014;8(6):6440-8.
90. Bardeen J. Electrical Conductivity of Metals. J Appl Phys. 1940;11(2):88-111.
91. Yang Y, Park J, Kwon SH, Kim YS. Fluidic Active Transducer for Electricity Generation. Sci Rep. 2015;5:15695.
92. Song Y, Chen H, Su Z, Chen X, Miao L, Zhang J, et al. Highly Compressible Integrated Supercapacitor–Piezoresistance-Sensor System with CNT–PDMS Sponge for Health Monitoring. Small. 2017;13(39):1702091.
93. Jung S, Lee J, Hyeon T, Lee M, Kim D-H. Fabric-Based Integrated Energy Devices for Wearable Activity Monitors. Adv Mater. 2014;26(36):6329-34.
94. Liang Y, Zhao F, Cheng Z, Zhou Q, Shao H, Jiang L, et al. Self-powered wearable graphene fiber for information expression. Nano Energy. 2017;32:329-35.
95. Liang J, Tong K, Pei Q. A Water-Based Silver-Nanowire Screen-Print Ink for the Fabrication of Stretchable Conductors and Wearable Thin-Film Transistors. Adv Mater. 2016;28(28):5986-96.
96. Huang Y, Li H, Wang Z, Zhu M, Pei Z, Xue Q, et al. Nanostructured Polypyrrole as a flexible electrode material of supercapacitor. Nano Energy. 2016;22:422-38.
97. Zou H, Zhang Y, Guo L, Wang P, He X, Dai G, et al. Quantifying the triboelectric series. Nat Commun. 2019;10(1):1427.
98. Wang S, Xie Y, Niu S, Lin L, Liu C, Zhou YS, et al. Maximum surface charge density for triboelectric nanogenerators achieved by ionized-air injection: methodology and theoretical understanding. Adv Mater. 2014;26(39):6720-8.
99. Cheng G-G, Jiang S-Y, Li K, Zhang Z-Q, Wang Y, Yuan N-Y, et al. Effect of argon plasma treatment on the output performance of triboelectric nanogenerator. Appl Surf Sci. 2017;412:350-6.
100. Zhang B, Zhang L, Deng W, Jin L, Chun F, Pan H, et al. Self-Powered Acceleration Sensor Based on Liquid Metal Triboelectric Nanogenerator for Vibration Monitoring. ACS Nano. 2017;11(7):7440-6.

101. Yang Y, Sun N, Wen Z, Cheng P, Zheng H, Shao H, et al. Liquid-Metal-Based Super-Stretchable and Structure-Designable Triboelectric Nanogenerator for Wearable Electronics. ACS Nano. 2018;12(2):2027-34.
102. Helseth LE, Guo XD. Hydrophobic polymer covered by a grating electrode for converting the mechanical energy of water droplets into electrical energy. Smart Mater Struct. 2016;25(4).
103. Liang X, Jiang T, Liu G, Xiao T, Xu L, Li W, et al. Triboelectric nanogenerator networks integrated with power management module for water wave energy harvesting. Adv Funct Mater. 2019;29(41).
104. Wei A, Xie X, Wen Z, Zheng H, Lan H, Shao H, et al. Triboelectric Nanogenerator Driven Self-Powered Photoelectrochemical Water Splitting Based on Hematite Photoanodes. ACS Nano. 2018;12(8):8625-32.
105. Li Z, Chen J, Guo H, Fan X, Wen Z, Yeh MH, et al. Triboelectrification-Enabled Self-Powered Detection and Removal of Heavy Metal Ions in Wastewater. Adv Mater. 2016;28(15):2983-91.
106. Nie J, Ren Z, Shao J, Deng C, Xu L, Chen X, et al. Self-Powered Microfluidic Transport System Based on Triboelectric Nanogenerator and Electrowetting Technique. ACS Nano. 2018;12(2):1491-9.
107. Vo CP, Shahriar M, Le CD, Ahn KK. Mechanically active transducing element based on solid–liquid triboelectric nanogenerator for self-powered sensing. Int J Pr Eng Man-GT. 2019;6(4):741-9.
108. Schwartz G, Tee BC, Mei J, Appleton AL, Kim DH, Wang H, et al. Flexible polymer transistors with high pressure sensitivity for application in electronic skin and health monitoring. Nat Commun. 2013;4:1859.
109. 109. Wang C, Hwang D, Yu Z, Takei K, Park J, Chen T, et al. User-interactive electronic skin for instantaneous pressure visualization. Nat Mater. 2013;12(10):899-904.
110. Someya T, Sekitani T, Iba S, Kato Y, Kawaguchi H, Sakurai T. A large-area, flexible pressure sensor matrix with organic field-effect transistors for artificial skin applications. Proceedings of the National Academy of Sciences of the United States of America. 2004;101(27):9966.
111. Shi Q, Wang H, Wang T, Lee C. Self-powered liquid triboelectric microfluidic sensor for pressure sensing and finger motion monitoring applications. Nano Energy. 2016;30:450-9.
112. Shi Q, Wang H, Lee C. Using Water as A Self-Generated Triboelectric Sensor for Pressure and Flow Rate Measurement. Conference on Nano/Micro Engineered and Molecular Systems. Los Angeles, USA: April 9-12; 2017.
113. Wang Z, Wan D, Fang R, Yuan Z, Zhuo K, Wang T, et al. Water-based triboelectric nanogenerator for wireless energy transmission and self-powered communication via a solid-liquid-solid interaction. Appl Surf Sci. 2022;605:154765.
114. Xiong J, Luo H, Gao D, Zhou X, Cui P, Thangavel G, et al. Self-restoring, waterproof, tunable microstructural shape memory triboelectric nanogenerator for self-powered water temperature sensor. Nano Energy. 2019;61:584-93.
115. Zhang X, Yu M, Ma Z, Ouyang H, Zou Y, Zhang SL, et al. Self-Powered Distributed Water Level Sensors Based on Liquid–Solid Triboelectric Nanogenerators for Ship Draft Detecting. Adv Funct Mater. 2019;29(41):1900327.
116. Wang Y, Wang Z, Zhao D, Yu X, Cheng T, Bao G, et al. Flow and level sensing by waveform coupled liquid-solid contact-electrification. Materials Today Physics. 2021;18:100372.
117. Mosadegh B, Polygerinos P, Keplinger C, Wennstedt S, Shepherd RF, Gupta U, et al. Pneumatic Networks for Soft Robotics that Actuate Rapidly. Adv Funct Mater. 2014;24:2163-70.
118. 118. Shahriar M, Vo CP, Ahn KK. Self-powered flexible PDMS channel assisted discrete liquid column motion based triboelectric nanogenerator (DLC-TENG) as mechanical transducer. Int J Pr Eng Man-GT. 2019;6(5):907-17.
119. Li X, Yeh MH, Lin ZH, Guo H, Yang PK, Wang J, et al. Self-Powered Triboelectric Nanosensor for Microfluidics and Cavity-Confined Solution Chemistry. ACS Nano. 2015;9(11):11056-63.
120. Zhang H, Yang Y, Su Y, Chen J, Hu C, Wu Z, et al. Triboelectric nanogenerator as self-powered active sensors for detecting liquid/gaseous water/ethanol. Nano Energy. 2013;2(5):693-701.
121. Zhang W, Wang P, Sun K, Wang C, Diao D. Intelligently detecting and identifying liquids leakage combining triboelectric nanogenerator based self-powered sensor with machine learning. Nano Energy. 2019;56:277-85.
122. Choi D, Tsao Y-H, Chiu C-M, Yoo D, Lin Z-H, Kim DS. A smart pipet tip: Triboelectricity and thermoelectricity assisted in situ evaluation of electrolyte concentration. Nano Energy. 2017;38:419-27.
123. Jiang P, Zhang L, Guo H, Chen C, Wu C, Zhang S, et al. Signal Output of Triboelectric Nanogenerator at Oil-Water-Solid Multiphase Interfaces and its Application for Dual-Signal Chemical Sensing. Adv Mater. 2019;31(39):e1902793.